GENETIC ABLATION OF THE PLATELET ACTIVATING FACTOR RECEPTOR DOES NOT IMPAIR LEARNING AND MEMORY IN WILD-TYPE MICE OR ALTER AMYLOID PLAQUE NUMBER IN A TRANSGENIC MODEL OF ALZHEIMER"S DISEASE

Vian Peshdary

Thesis submitted to the Department of Biochemistry, Microbiology, and Immunology
in partial fulfillment of the requirements for the degree of Masters in Science

University of Ottawa
Ottawa, Ontario, Canada
December, 2011

© Vian Peshdary, Ottawa, Canada, 2012

ABSTRACT

We have recently established that aberrant alkylacylglycerophosphocholine metabolism results in the increased tissue concentration of platelet activating factors (PAFs) in the temporal cortex of Alzheimer Disease (AD) patients and in TgCRND8 mice over-expressing mutant human amyloid precursor protein. PAF lipids activate a G-protein coupled receptor (PAFR) reported to be expressed by microglia and subsets of neurons in rat. It is not known whether this same expression pattern is recapitulated in mice however, as the expression has only been inferred by use of pharmacological PAFR antagonists, many of which impact on both PAFR-dependent and PAFR-independent signalling pathways. PAFR plays a role in long term potentiation (LTP) induction in rats. PAFR has also been implicated in behavioural indices of spatial learning and memory in rats. Contradictory reports using mice provide ambiguity regarding the role of PAFR in LTP induction in mice. To assess whether PAFR is expressed in murine neurons, I localized PAFR mRNA in wild-type C57BL/6 mice using PAFR KO mice as a negative control. I further showed that the loss of PAFR did not impair learning and memory although this assessment must be considered preliminary as the behavioural test employed was not optimized to detect changes in learning and memory of C57BL/6 mice over time adequately. Finally, I showed that the loss of PAFR in TgCRND8 mouse model of AD had no impact upon Aβ plaque number. My observations suggest that PAFR is restricted to microglial-like cells in mouse hippocampus and as such, it may not play a role in learning and memory.

ACKNOWLEDGMENTS

I warmly thank my supervisor, Dr. Steffany A.L. Bennett for allowing and helping me learn valuable science and life lessons. I cannot express my appreciation and immense gratitude towards Dr. Bennett for her patience and understanding for all the times that I had family emergencies, as there were quite a bit of them. I would like to also thank my lab-mates for all the mentorships of various techniques and continuous support they have provided me. I thank Dr. Odette Laneuville and Dr. Ruth Slack for being members of my TAC committee. I further thank Dr. Odette Laneuville for her mentorship and guidance. Last but not least, I thank the Canadian Institutes of Health Research (CIHR) for providing funding for our lab and my research as grants provided to Dr. Steffany Bennett.

TABLE OF CONTENTS

TABLE OF CONTENTS

TABLE OF CONTENTS

TABLE OF CONTENTS

LIST OF ABBREVIATIONS

ABCB1	ATP-binding-cassette transporter
Ab AC AD	Amyloid beta
AC	Anterior cortex
AD	Alzheimer disease
AP-1	Activator protein 1
APP	Amyloid precursor protein
BBB	Blood-brain barrier
BF	Basal Forebrain
Bp	Base pair
CA	*CornuAmmonis*
cAMP	Cyclic adenosine monophosphate
CaMKII	Calcium/calmodulin-dependent protein kinase II
cDNA	Complementary deoxyribonucleic acid
CNS	Central nervous system
Ctx	Cerebral cortex
DIG	Digoxin
DAG	Diacylglycerol
dNTPs	deoxyribonucleotide triphosphates
ERK	Extracellular signal-regulated kinases
EOFAD	Early onset familial Alzheimer disease
EPSPS	Excitatory postsynaptic potential
FAD	Familial Alzheimer disease
FACS	Fluorescence activated cell sorting
fi	fimbria
GL	Granular layer
GAPDH	Glyceraldehyde 3-phosphate dehydrogenase
H	Hippocampus
HPF	Hippocampal formation
Inr	Initiator sequence
IP	Intraperitoneal
IP3	Inositol 1, 4, 5,- triphosphate
KO	Knock out
LOAD	Late onset Alzheimer disease
LPCAT	Lysophosphatidylcholineacyltransferase
LTP	Long term potentiation
MAPK	Mitogen-activated protein kinase
MDR1 Pgp	Human multidrug-resistance 1 P-glycoprotein
ML	Molecular layer

LIST OF ABBREVIATIONS

MM	Master mix
mo	Stratum molecular
MWM	Morris water maze
mRNA	Messenger ribonucleic acid
NF-H2O	Nuclease free water
NF-κB	Nuclear factor kappa-B
NFT	Neurofibrillary tangles
NMDAR	N-Methyl-D-aspartate receptor
NonTg	None transgenic
ORF PAF	Open reading frame
PAFR	Platelet activating factor
PC	Platelet activating factor receptor
PCR	Posterior cortex
PGK	Polymerase chain reaction
PI3K	Phosphoglycerate kinase
PKC	Phosphatidylinositol 3-kinase
PL	Protein kinase C
PMN	Phospholipase Purkinje layer
PSEN	polymorphonuclear neutrophils
PTAFR	Presenilin
RNA	Platelet activating factor receptor gene
RT-PCR	Ribonucleic acid
sAPP	Reverse transcription polymerase chain reaction
Sg	Soluble amyloid precursor protein
Slm	Stratum granulosum Stratum lacunosum
Slu	Stratum lucidem
So	Stratum oriens
Sp-1	Specificity protein 1
Sr	Stratum radiatum
TdT	Terminal deoxynucleotidyltransferase gene
Tg	Transgenic
Thal	Thalamus
VO	Ventro orbital cortex
WT	Wild-type

LIST OF FIGURES

LIST OF TABLES

Chapter 1

INTRODUCTION

Platelet Activating Factor (PAF) - PAF (1-*O*-alkyl-2-acetyl-*sn*-glycero-3-phosphocholine) is a member of the ether-linked alkylacylglycerophospholipid family. The PAF family is characterized by an alkyl ether linkage at the *sn*-1 position, a short fatty acid chain at the *sn*-2 position, and can exhibit one of the following three head groups at the *sn*-3 position: phosphocholine, phosphoethanolamine or phosphatidic acid. The most common PAF species is PAF which consists of a hexadecyl (16:0) chain at the *sn*-1 position, an acetyl group at the *sn*-2 position, and phosphocholine head group at the *sn*-3 position (Figure 1).

PAF Biosynthesis: the Remodelling and the *De Novo* Pathways - PAF is synthesized through two main pathways, the remodelling pathway and the *de novo* pathway (Figure 2). Both of these pathways include distinct enzymatic activities. The remodelling pathway is largely involved in metabolism of PAF by stimulated inflammatory cells (Alonso et al., 1982; Lee et al, 1984; Ninio et al, 1982). In this pathway, calcium-sensitive cytoplasmic phospholipase A_2 (cPLA$_2$) hydrolyses the membrane phospholipid 1-alkyl-2-arachidonyl-glycero-phosphocholine (AAGPC) at the *sn*-2 position to generate the precursor of PAF, alkyllyso-PAF (*lyso*-PAF with a hydroxyl group at the *sn*-2 position) and to release arachidonic acid (AA). *Lyso*-PAF then acts as a substrate for the enzyme, lysophosphatidylcholine acyltransferase

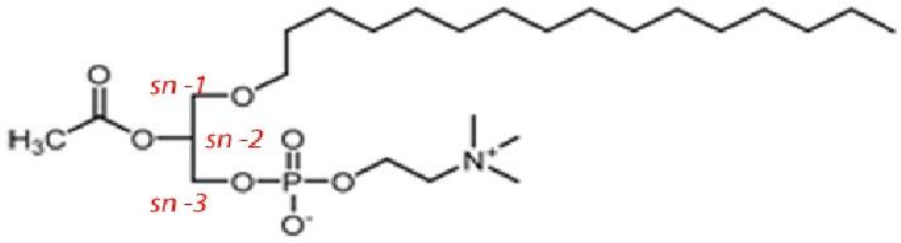

Figure 1. The Molecular Structure of Platelet Activating Factor. The glycerol backbone is denoted by the three carbon positions as *sn-1*, *sn-2*, and *sn-3* depicting alkyl group with ether linkage, acetyl moiety and a phosphocholine head group respectively.

(LPCAT) which catalyzes the transfer of the acetyl moiety from acetyl CoA to the hydroxyl group at the *sn*-2 position, releasing water (H_2O) (Prescott et al., 2000). The *de novo* pathway promotes regulation of physiological levels of PAF and is involved mainly in cells of the liver, spleen, kidney, reproductive organs, and brain (Bussolino et al., 1986; Renooij and Snyder, 1981; Snyder et al., 1987; Snyder et al., 1995). This pathway involves the acetylation of 1-alkyl glycerolphosphate (lysophosphatidic acid), that is then converted to 1-alkyl-2-acetyl-glycerophosphate, who is in turn converted to 1-alkyl-2-acetylglycerol and finally to PAF by dithiothreitol-insensitive: cholinephosphotransferase (Figure 2) (Renooij and Snyder, 1981).

PAF Translocation: From Site of Synthesis to Cell Surface - Significant amount of synthesized PAF are secreted to the extracellular milieu, while lesser amounts remain associated with the cell membrane (Prescott, 2002). It should be noted that PAF must interact with its cell surface receptor (PAFR) in order to transduce diverse signals leading to cell stimulation. Although we and others have shown that PAF lipids can also signal through PAFR-independent pathways, the majority of physiological events are attributed to the activation of PAFR (Ryan et al., 2007; Tokuoka et al., 2003; Dyer et al., 2010; Wang et al., 1999). As such, the translocation of PAF from the site of its synthesis to the cell surface is of interest. Research has proposed convincing evidence that the human multidrug-resistance (MDR1) P-glycoprotein (Pgp), an ATP-binding-cassette transporter (ABCB1) may play a significant role in the secretion and better yet, direct translocation of PAF across the plasma membrane (Ernest and Bello-Reuss, 1999; Raggers et al., 2001).

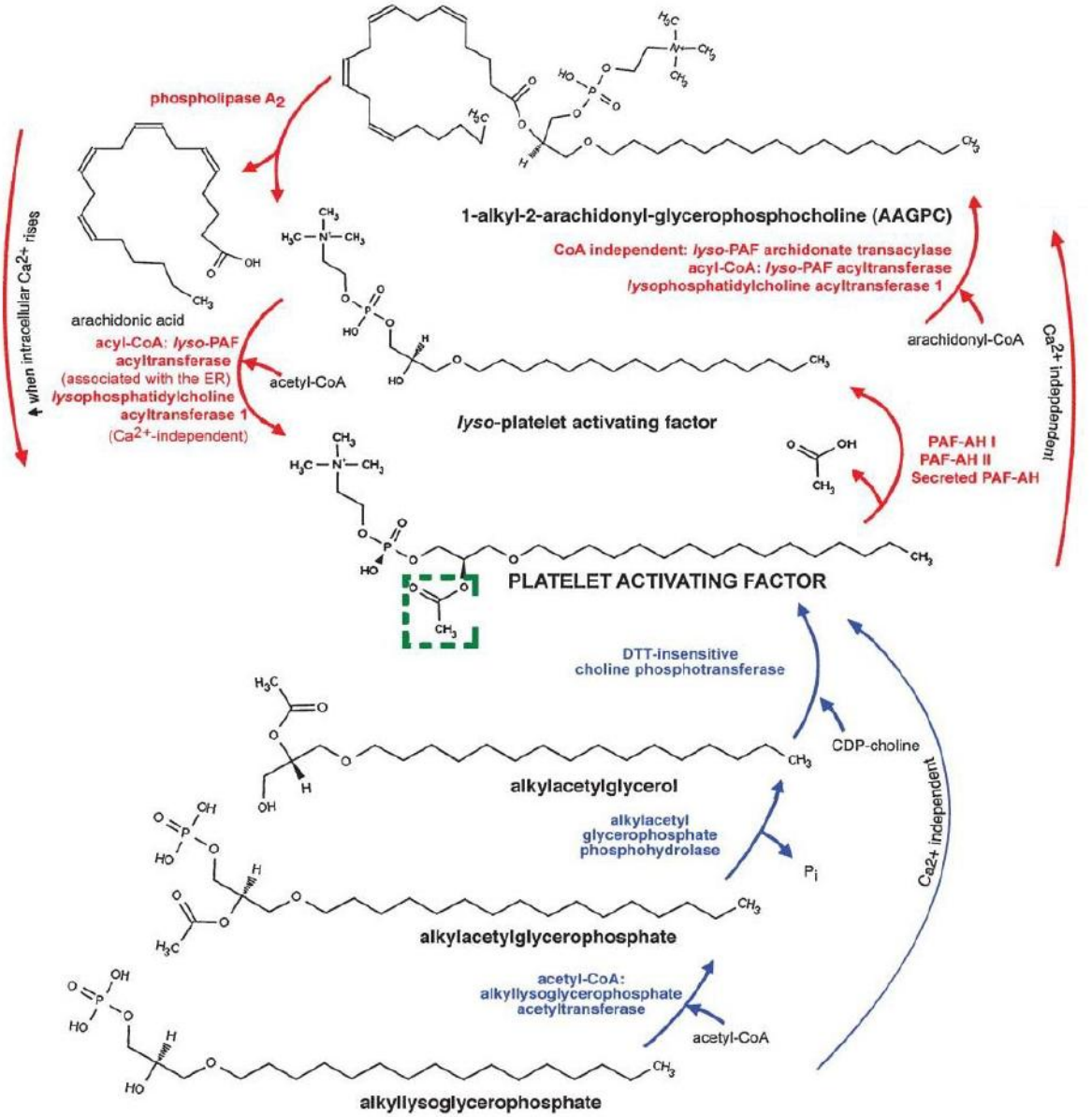

Figure 2. **PAF Biosynthesis: the Remodelling and the *De Novo* Pathways.** A schematic diagram illustrating two metabolic pathways of platelet activating factor (PAF). The remodelling pathway is depicted in red and the *de novo* pathway is depicted in blue. This figure was adapted from Ryan et al., 2008.

This thought is rather plausible since MDR1 Pgp is ubiquitously expressed in virtually all cells and it can recognize short-chain analogues of phosphatidylcholine (PC) and lipids with shortened acyl chains (van Helvoort et al., 1996; Raggers et al., 2001). Also, several ATP-binding cassette (ABC) proteins are thought to act as lipid lipases, which may be involved in PAF translocation (Borst et al., 2000).

PAF as a Bioactive Lipid Mediator - PAF is a potent bioactive phospholipid mediator. As a glycerophosphocholine second messenger, PAF promotes activation of many cell types including neurons, astrocytes, microglia, oligodendrocytes, polymorphonuclear neutrophils (PMN), basophils, eosinophils, platelets, leukocytes, endothelial cells, monocytes/ macrophages, and smooth muscle cells (Montrucchio et al., 2000; Aihara et al., 2000; Lotner et al., 1980; Brattond and Henson, 1989; Camussi et al., 1990; Triggiani et al., 1991; O"Neil et al., 1992 ; Blank et al., 1979 ; Kunievsky et al., 1994). Appropriate stimuli, particularly those involved in inflammation lead to the synthesis and release of PAF from neural as well as non neural cell types (Montrucchio et al., 2000). It must be noted that the interaction of PAF with non-neural cells, particularly those involved in inflammatory response mediate diverse biological processes including: wound healing, angiogenesis, reproduction, physiological inflammation, and apoptosis (Montrucchio et al., 2000). In fact, the term *PAF* was coined in 1972 by Benveniste *et al.* for the lipid mediator released from rabbit basophils after IgE stimulation that was responsible for platelets aggregation (Benveniste et al., 1972).

The diverse effects of PAF are also evident in the central nervous system (CNS). In the CNS, physiological concentrations (1-100 nM) of PAF induce pro-inflammatory and neuromodulating effects (Prescott et al., 2000; Farooqui et al., 2008). PAF promotes neuronal differentiation and has been implicated in synaptic plasticity and memory formation (Clark et al., 1992; Izquierdo et al., 1995; Bazan et al., 1997). Also in the brain, PAF is associated with gene expression, nociception, calcium mobilization, neuronal cell migration, and long term potentiation (LTP) (Farooqui et al., 2008). Moreover, during LTP, a component underlying synaptic plasticity, PAF may act as a retrograde messenger in the CA1 region of the hippocampus (Kato et al., 1994). Also, Moriguchi *et al.* have recently demonstrated that in the CA1 region of the hippocampus in rat, PAF affects synaptic strength through activation of protein kinases leading to consolidation of LTP (Moriguchi et al., 2010). Taken together, PAF can be considered as one of the most potent and versatile lipid mediators found in mammals (Prescott et al., 2000). These effects are attributed to PAF acting by binding to a specific G protein-coupled seven transmembrane domains receptor (PAFR) mediating intracellular signal transduction.

Platelet Activating Factor Receptor (PAFR): From Gene to Protein - PAFR is a member of the rhodopsin family of G protein-coupled receptor with seven transmembrane spanning domains (Figure 3A). The first PAFR cDNA was purified from a guinea-pig lung cDNA library using an expression cloning method (Honda et al., 1991). The human *PTAFR*‡ gene structure is composed of only three exons; two

‡ In this thesis, I will use the acronym PAFR to refer to the protein and transcript and *PTAFR* (gene name) to refer only to PAFR gene.

Figure 3. *Platelet Activating Factor Receptor (PTAFR)* Gene and Protein Structure. A, depicting a schematic representation of PAFR protein structure. Circle indicate amino acid residues. A disulphide bond between cysteine residues in the first and second extracellular loops is illustrated by a line. B, depicting the *PTAFR* gene structure.The *PTAFR* gene is composed of three exons; two of which are 5' noncoding exons and the third 3‟-exon holds the entire open reading frame. Each of the 5'-noncoding exons has distinct transcriptional initiation sites (promoter 1 and 2), and can be alternatively spliced at a common splice acceptor site on the 3‟ coding exon - yielding two of four different functional transcripts (transcript 1 and 2). (This figure was adapted from Ishii and Shimizu, 2000).

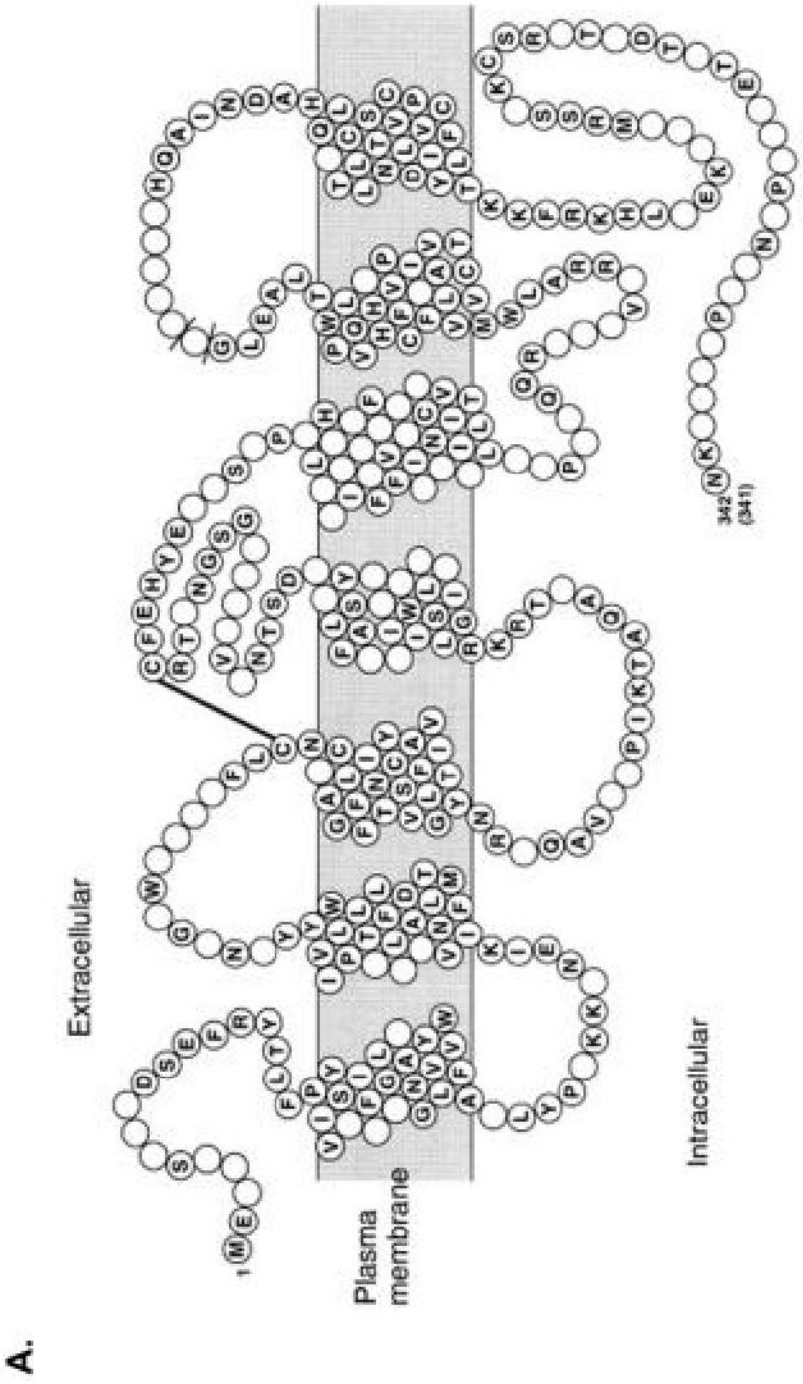
A.
Extracellular
Plasma membrane
Intracellular
1
342 (341)

B.

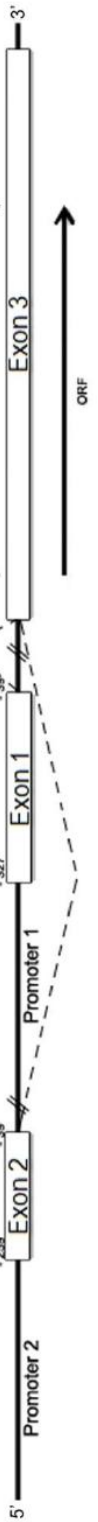
3'
1029
TAG
Exon 3
ORF
1
ATG
-39
Exon 1
-327
Promoter 1
-39
Exon 2
-259
Promoter 2
5'

of which are 5'-noncoding exons and the third 3'-exon holds the entire coding sequence (Figure 3B). A large intron separates exons 1 and 2, although exon 2 is upstream of exon 1 (Kotelevets et al., 1998). It was originally reported by Mutoh *et al.* that each of the 5'-noncoding exons has distinct transcriptional initiation sites (promoter 1 and 2), and can be alternatively spliced at a common splice acceptor site on the 3' coding exon - yielding two different functional transcripts (transcript 1 and 2) (Mutoh et al., 1993). Recently two other functional transcripts of human *PTAFR* gene have been reported contributing to a total of 4 functional transcripts. All 4 different splice variants however encode the same PAFR protein. The two promoters, 1 and 2 lack the TATA and CCAAT box. Instead, promoter 1 has consensus sequences for transcription factor nuclear factor kappa-B (NF-κB), specificity protein 1 (Sp-1), and the Initiator (*Inr*) sequence homologous to the murine *terminal deoxynucleotidyltransferase* gene (TdT) (Mutoh et al., 1993; Smale and Baltimore, 1989; Smale et al., 1990). Promoter 2 consist of consensus sequences for transcription factor activator protein 1 (AP-1), AP-2, and Sp-1 (Mutoh et al., 1993). To date, only the expression of transcript 1 and 2 have been characterized. Both transcript 1 and 2 are expressed in heart, lung, spleen, and kidney; whereas transcript 1 is also detected in differentiated human eosinophilic cell line (EoL-1 cells), polymorphonuclear, neutrophils (PMN), eosinophils, peripheral leukocytes, monocytes, and brain (Mutoh et al., 1993; Kotelevets et al., 1998; Kishimoto et al., 1996; LeVan et al., 1998; Shimada et al., 1998; Ishii and Shimizu, 2000). As such, it has been suggested that the existence of two different promoters may yield regulatory control of *PTAFR* gene expression specific to various cells and tissues (Ishii and Shimizu, 2000).

The overall sequence homology of PAFR protein among different species (human, guinea-pig, rat, and mouse) is 72%, although it should be noted that mouse to rat sequence homology is as high as 91% (Ishii and Shimizu, 2000). PAFR is post transcriptionally modified by a putative disulphide bond between cysteine residues in the first and second extracellular loops. Also, human PAFR contains a single N linked consensus glycosylation (N-glycosylation) sequence found in the second extracellular loop with no other major posttranscriptional modifications. Unlike the human PAFR, the cloned PAFRs of other species (guinea-pig, rat, and mouse) all have an additional N-glycosylation at the N-terminus (Honda et al., 1991; Bito et al., 1994; Ishii and Shimizu, 2000). It has been reported that the human N-glycosylation has a significant role in facilitating the expression of PAFR to the cell surface membrane (García et al., 1995). This is interesting since generally carbohydrate moieties of glycolproteins are thought to be important for intracellular trafficking and cell surface expression (Rademacher et al., 1988). Furthermore, the C-terminus of PAFR includes several serine and threonine residues that are subject to phosphorylation upon PAF binding, an event that facilitates PAFR internalization and desensitization (Takano et al., 1994).

PAFR Distribution - Radio labelled (tritium) PAF agonists and PAFR antagonists have been used to localize PAFR in many cells and tissues. The binding studies performed using intact cells have exhibited specific binding capacity to PAF inmacrophages, neutrophils, platelets, mononuclear leukocytes, Kupffer cells, umbilical vein endothelial cells, and tracheal or bronchial epithelial cells (Chao and Olson, 1993; Korth et al., 1995; Herbert et al., 1992; LeVan et al., 1998; Ishii and

Shimizu, 2000). However, other studies using only the plasma membrane fractions of cells have also successfully shown PAF binding ability to a receptor. These tissues include kidney, lung, spleen, liver, myometrium, ileum, epidermoid cells, and brain (Takano et al., 1991; Hwang et al., 1985; Hwang et al., 1987; Zhu et al., 1992; Hwang et al., 1983; Travers et al., 1995; Bito et al., 1992; Marcheselli et al., 1990). Moreover, PAFR mRNA expression in different cells and tissues has also been pursued by various groups. Northern blot experiments have been used to localize PAFR mRNA expression in various organs of human, guinea-pig, rat, and mouse. In humans, PAFR mRNA expression has been found in neutrophils, monocyte-derived dendritic cells, placenta, monocytes, lung, and umbilical vein endothelial cells (Kunz et al., 1992; Ye et al., 1991; Thivierge et al., 1993; Ouellet et al., 1994; Shirasaki et al., 1994; Thivierge et al., 1996; Sozzani et al., 1997; Dagenais et al., 1997; Ishii and Shimizu, 2000). However no detection was evident in the heart, skeletal muscle, liver, pancreas, kidney, and brain, although there are reports of cloning of PAFR cDNA from the heart (Sugimoto et al., 1992). This slight controversy may be subject to the limited sensitivity of Northern blotting in detecting mRNA expression. Furthermore, PAFR mRNA expression in guinea-pig is largely abundant in leukocytes, although noticeable detection is evident in lung, spleen, and kidney; whereas no signal were detected in liver, small intestine, brain, and heart. In rat, PAFR mRNA was detected in spleen, small intestine, liver, kidney, heart, lung, brain, microglia, skin, and mesangial cells and much less in skeletal muscle, stomach, thymus, adrenal, pancreas, and testis (Honda et al., 1991; Bito et al., 1994; Hwang et al., 1985; Mutoh et al., 1996; Mori et al., 1996; Nakao et al., 1997). Moreover, in mice the expression of PAFR was highly abundant in peritoneal macrophages.

Murine spleen was reported to be the most abundant organ in PAFR mRNA expression followed by small intestine, heart, skeletal muscle, liver, lung, kidney, and brain (Ishii et al., 1996). It should not pass unnoticed that there is a definite tissue specific as well as species specific regulatory mechanisms underlying PAFR mRNA expression.

PAF Interaction with PAFR - It is widely accepted that the diverse intracellular events signalled by PAF are due to the interaction of PAF with PAFR. As described previously, PAF consists of a glycerol backbone, where at the first carbon, denoted as *sn*-1 position there is an alkyl group with an ether linkage. At the second carbon, *sn*-2 position is an acetyl moiety, and at the third carbon, *sn*-3 position there is a phosphocholine head group. All of these unique features of PAF allow the interaction with PAFR and the subsequent signalling within the cell. The ether linkage at the *sn*-1 position promotes PAF recognition by PAFR; where the length and degree of saturation of the alkyl chain elicit the activation of different PAFR signalling pathways (Handa et al., 1991; Carolan et al., 1990; Erger et al., 1996; Stoddart et al., 2001). PAF is also recognized via its acetyl moiety at the *sn*-2 position, as the short length of the acetyl group promotes PAF affinity to PAFR. Thus extension by any more than one methyl group renders PAFR activity lowered by 10 - to 100 - fold (Prescott et al., 2000; Tanaka et al., 1994; Blank et al., 1982). Finally, PAFR identifies PAF by the phosphocholine head group at the *sn*-3 position (Prescott et al., 2000; O'Flaherty et al., 1994; Carolan et al., 1990; Hwang et al., 1989; Ishii et al., 1997). The latter is based on alanine scanning mutagenesis experiments carried by Ishii *et al.* in 1997 where they concluded that the imidazole groups of three histidine residues in

transmembranes five and six form a polar pocket. Thus, they hypothesized that this polar pocket is where the phosphocholine head group of PAF may bind (Ishii et al., 1997). Furthermore, it has been reported that substitution of phosphocholine by phosphoethanolamine reduces binding affinity of PAF to PAFR (O'Flaherty, 1994). It is of significance to note that any alterations to these structures of PAF may affect PAFR signalling (Prescott et al., 2000).

Intracellular Signal Transduction of PAFR - Signal transduction occurs once an extracellular signalling molecule, in this case PAF, activates a membrane receptor PAFR who then elicits multiple intracellular signalling pathways. PAFR activation by PAF leads to GTPase activation, signalling through $G\alpha_o$, $G\alpha_i$, $G\beta\gamma$, and $G\alpha_q$ (Honda et al., 1991; Clrak et al., 2000; Farooqqui et al., 2008). Generally, this signalling results in phospholipid turnover via phospholipases C, D and A_2 pathways, protein kinase C and tyrosine kinase activation (Shukla et al., 1992). Within inflammatory cell types, PAFR has been shown to couple to either Gi or Gq (Brown et al., 2006). Moreover, PAFR activation favours calcium influx via receptor operated channels. Also, as Shukla reviewed, these multiple signalling pathways play a role in PAF induced expression of primary response genes (Shukla et al., 1992). Although we and others have shown that PAF lipids can also signal through PAFR-independent pathways, the majority of physiological events are attributed to the activation of PAFR (Ryan et al, 2007; Tokuoka et al., 2003; Dyer et al., 2010; Wang et al., 1999).

PAFR-mediated intracellular signal transduction evokes second messengers

including, calcium, cyclic adenosine monophosphate (cAMP), diacylglycerol (DAG), and inositol 1, 4, 5,-triphosphate (IP3) (Ishii and Shimizu, 2000). PAFR-mediated intracellular signal transduction also leads to cascade of kinase activations include mitogen-activated protein kinase (MAPK), phosphatidylinositol 3-kinase (PI3K), protein tyrosine kinases, protein kinase C (PKC), and G-protein receptor kinase (Figure 4) (Chao et al., 1993; Izumi and Shimizu, 1995; Ishii and Shimizu, 2000). In the family of MAPK, the two classes that are phosphorylated from PAFR signalling are p38 and extracellular signal-regulated kinases (ERKs). There are many reports indicating that there may be multiple pathways involved in activating MAPK as a result of PAFR signalling, depending on cell type or species (Franklin et al., 1993; Honda et al., 1994; van Biesen et al., 1996; Ishii and Shimizu, 2000).

In rat brain, PAFR expression has been localized to a subset of neurons and glia with predominant expression by microglia (Mori et al., 1996). In rat hippocampal CA1 neurons, PAF has been shown to induce synaptic facilitation by interacting with PAFR and activating calcium/calmodulin-dependent protein kinase II (CaMKII), protein kinase C (PKC) and extracellular signal-regulated kinase (ERK) (Moriguchi et al., 2010). Moreover, PAFR activation by PAF lipids has been implicated in promoting spatial learning and memory in rats (Teather et al., 1998). In rat microglia, PAFR downstream targets include inositol phospholipid turnover, calcium signals and activation of ERK mitogen-activated protein (MAP) kinase leading to PAF induced chemotaxis and gene expression (Wang et al., 1999; Righi et al., 1995).

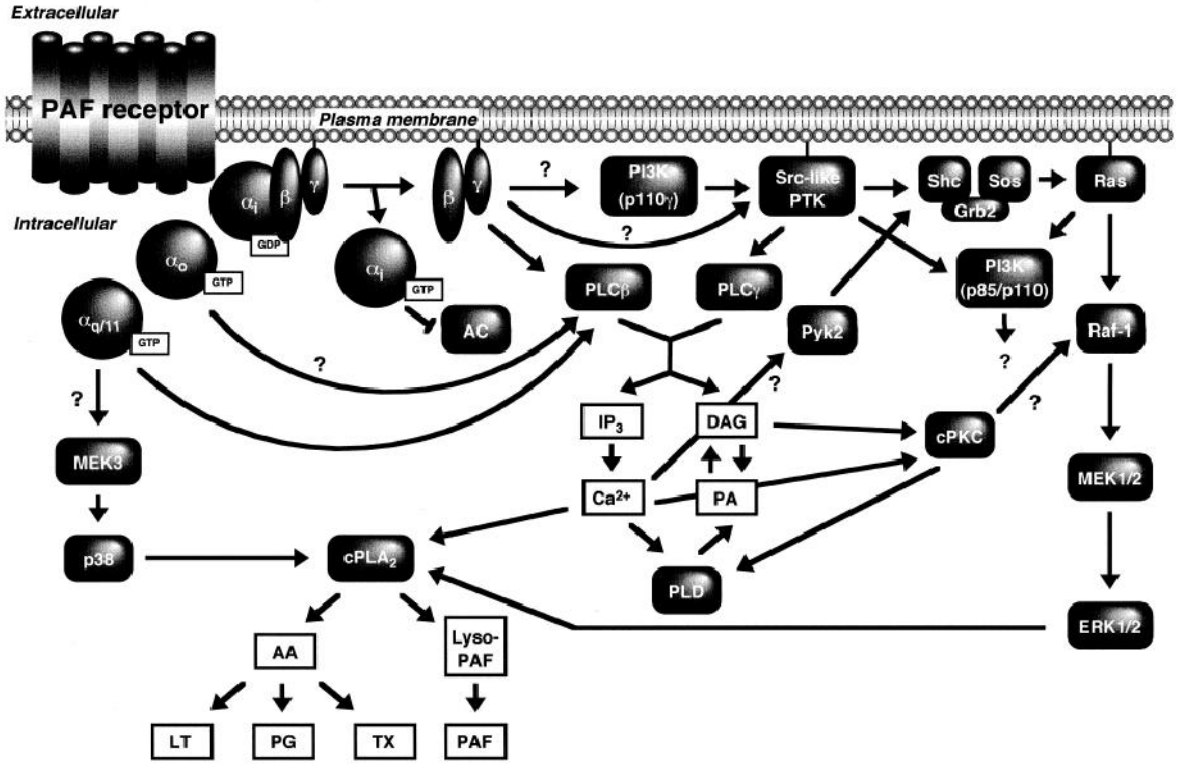

Figure 4. Platelet Activating Factor Intracellular Signal Transduction Pathways. Schematic diagram depicting the intracellular signalling events coupled to PAFR. PAFR activation by PAF leads to GTPase activation, signalling through $G\alpha_o$, $G\alpha_i$, $G\beta\gamma$, and $G\alpha_q$. These signalling results in phospholipid turnover via phospholipases C, D and A_2 pathways, protein kinase C and tyrosine kinase activation. Second messengers including, calcium, cyclic adenosine monophosphate (cAMP), diacylglycerol (DAG), and inositol 1, 4, 5,-triphosphate (IP3) are also upregulated upon PAFR activation. Finally, PAFR activation induces kinase activations such as, p38, extracellular signal-regulated kinases (ERKs), phosphatidylinositol 3 kinase (PI3K), protein tyrosine kinases, protein kinase C (PKC), and G-protein receptor kinase. Question marks indicate multiple or uncharacterized steps. (This figure was reproduced from and Shimizu, 2000).

PAFR in Hippocampus: Long Term Potentiation and Learning and Memory - Long term potentiation (LTP) is a long lasting enhancement of the effectiveness of synaptic transmission following a certain type of repeated stimulation (Farooqui et al., 2008). LTP is a form of synaptic plasticity which underlies learning and memory. LTP in the hippocampus can be induced in the CA1, CA3, and dentate gyrus regions. Induction of LTP by means of N-Methyl-D-aspartate receptor (NMDAR) activation elicits calcium influx, $cPLA_2$ activation and subsequently release of arachidonic acid (AA) (Bliss. and Collingridge, 1993; Farooqui et al., 2008). This postsynaptic event is believed to have an effect upon presynaptic cleft - mediated by retrograde messengers such as AA and nitric oxide (NO). These retrograde messengers are suggested to cross the synaptic cleft from the post synaptic neuron to the presynaptic neuron. One candidate for these retrograde messengers is suggested to be PAF (Ishii and Shimizu, 2000; Kato et al., 1994). Studies report that PAF may produce LTP in NMDAR dependent and independent ways and has been implicated in learning and memory (Wieraszko et al., 1993; Kato et al., 1994; Izquierdo et al., 1995). It must be noted however that all of these studies were performed on rat hippocampus and conclusions were derived from pharmacological approaches.

A study by Kobayashi *et al.* attempted to re-examine the potential role of PAF in LTP induction with a more specific approach using mice deficient in PAFR (PAFR KO) (Kobayashi et al., 1999; Ishii et al., 1998). Similar to the rat study by Kato *et al.*,Kobayashi‟s group conducted their electrophysiology experiments in the CA1

region of the hippocampus where the Schaffer collateral pathway was stimulated.

The rat electrophysiology study by Kato *et al.*, demonstrated that the administration of PAFR antagonist BN52021 blocked the enhancement of excitatory postsynaptic potentials (EPSP) in the CA1 region of rat hippocampus. Kobayashi *et al.*'s electrophysiology experiment in the CA1 region of mouse hippocampus on the other hand exhibited contradictory results. Kobayashi‟s group demonstrated that PAFR KO mice exhibited normal LTP in CA1 region of the hippocampus compared to wild type mice and did not display any irregularity in EPSP. In addition to using the PAFR KO mouse model, Kobayashi's group also used the same PAFR antagonist (BN52021) that was used in the rat study of Kato *et al.* Kobayashi's group demonstrated that unlike what was observed in the rat study, administration of the PAFR antagonist BN52021 on wild-type mice had no effect on LTP. As such, the findings of Kobayashi *et al*.'s electrophysiology experiments suggest that PAFR is not required for LTP induction in mouse hippocampus. This suggestion was later challenged as another study conducted by Chen *et al*. reported that LTP is attenuated in PAFR KO mice. Chen *et al.* used the same PAFR null mutant mice that were used by Kobayashi *et al.* and demonstrated that LTP is in fact attenuated in the dentate gyrus of the hippocampus (Chen et al., 2001). Chen *et al*. also utilized the BN52021 PAFR antagonist and were able to show that LTP is indeed attenuated in the dentate gyrus. The findings of Chen *et al.* elicit confusion regarding the role of PAFR in LTP induction and subsequently learning and memory in mice.

PAFR null Mutant (PAFR KO) Mouse Model - The generation of the PAFR null mutant (PAFR KO) mice has contributed immensely to PAFR research (Ishii et al., 1998). PAFR KO mice are the mouse model used in the studies of Kobayashi *et al.* and Chen *et al.* and were utilized in our studies as well. In the PAFR KO mouse model the PAFR open reading frame (ORF) has been disrupted with a PGK-neomycin cassette (Figure 5). The PAFR KO mice do not exhibit any obvious phenotypes. For example, they have no gross malformation in the brain, suggesting that PAF is unlikely to have a central physiological role in the development of the murine central nervous system (CNS). Furthermore, PAFR KO mice show severe attenuation in systemic anaphylactic responses such as, hypotension, heart rate change, lung edema, and lung resistance elevation with bronchoconstriction after antigen challenge. In fact, PAFR KO mice survived these systemic anaphylaxis compared to WT mice. These experiments suggest that PAF has a significant role in murine anaphylaxis. Moreover, PAFR KO mice have normal reproduction potential and no spontaneous abnormalities in the skin. Generally, from what has been reported, PAFR KO mice do not have any detectable physiological differences compared to wild-type mice (Isshi and Shimuzu, 2000; Ishii et al., 1998).

TgCRND8 Mouse Model of Alzheimer Disease - Another mouse model that has been utilized in my thesis is the TgCRND8 (Tg) mouse model of Alzheimer Disease (AD). This mouse model expresses a double mutant (KM670/671NL+V717F) form of the human amyloid precursor protein (APP) under the control of the prion cos-tet promoter (Chishti et al., 2001). This mouse model is a well-established model of AD, however as expected, not all clinical features are observed. In the TgCRND8 mice,

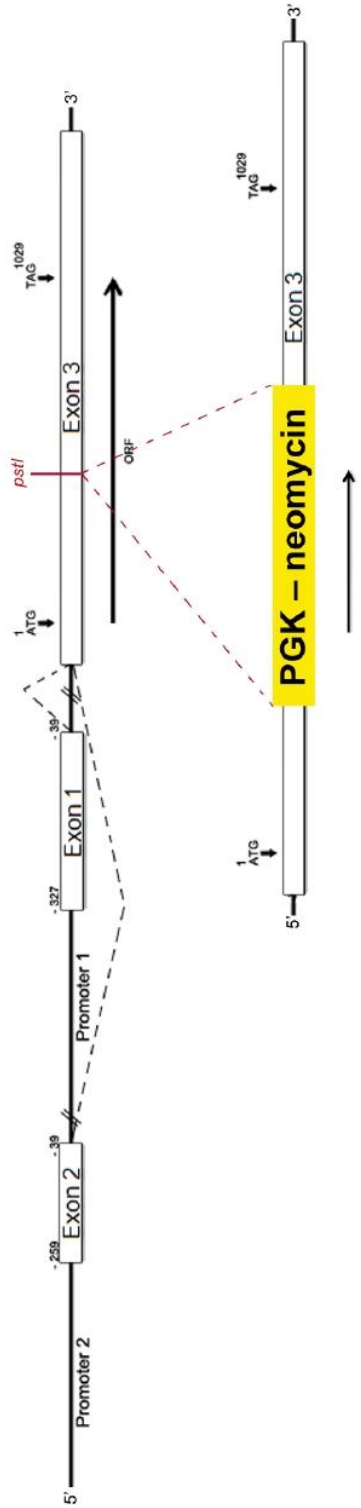

Figure 5. Disruption of the *PTAFR* Gene in Mice.At the top, the *PTAFR* gene is depicted. The third exon of *PTAFR* gene constitutes the entire open reading frame. The open reading frame is disrupted at the *PstI* restriction site as indicated. PGK neomycin cassette constitutes of PGK promoter (PGK-neo) and *neomycin resistance* gene with poly (A) signal. The direction of transcription for each gene is indicated by an arrow. This figure was adapted from Ishii and Shimizu, 2000; Ishii et al., 1998.

amyloid beta (Aβ) deposits are evident as early as three month of age, along with dense-core plaques and neuritic pathology that are visible from five months of age (Chishti et al., 2001). The TgCRND8 mice are impaired in acquisition and learning reversal as demonstrated by reference memory version of the Morris water maze (MWM) as early as three month of age (Chishti et al., 2001). Moreover, our lab has demonstrated that in the TgCRND8 mice, C16 PAF levels are elevated compared to the wild-type mice (Ryan et al., 2009). This is remarkable since this was evident also in the human AD brains compared to healthy human brains, suggesting that the TgCRND8 mice are able to exhibit similar human AD pathology (Ryan et al., 2009). It must be noted however that there are a few drawbacks in this model still. For instance, the survival rate of TgCRND8 is 50% - death occurs by 3 months of age (Chishti et al., 2001). In addition, the *APP* gene is driven by the prion cos-tet promoter, which leads to global Aβ accumulation in the brain synthesized by both neurons and glia as compared to neuron-specific production in human disease (Chishti et al., 2001). Moreover, as described previously, this promoter leads to constant rate of APP processing which results in equal Aβ deposition throughout the brain, while in human brain this is not the case. Although this animal model may not completely exhibit similar human AD pathology, it is one of the most widely used animal models for AD.

Alzheimer Disease (AD) - AD is a neurodegenerative disorder and the most common form of dementia (Wimo et al., 2010). AD-induced dementia is clinically described as a global decline of cognitive function - thinking, remembering and

reasoning - eventually resulting in death (National Institute of Aging Alzheimer's Disease Fact Sheet, 2011). AD cognitive decline is age dependent and progresses slowly, ultimately leaving the patient bedridden and in need of custodial care (Citron et al., 2004). There are two classifications of AD. One is the familial form of AD (FAD) with Mendelian inheritance of early onset (<60 years), otherwise known as early-onset FAD (EOFAD). The second form is *sporadic* AD attributed to individuals of 60 years or more of age, sometimes termed as late-onset AD (LOAD) (Bertram et al., 2010). Generally, EOFAD is caused by mutations in three distinct genetic loci identified by positional cloning; amyloid precursor protein (APP), presenilin 1 (PSEN1) and presenilin 2 (PSEN 2) (Tanzi et al., 2005). Although only <10% of AD cases have known genetic determinants, the exact mechanism underlying the nature of the non-genetic component constituting about 90% of the cases remains fairly unclear (Gatz et al., 2006). In addition, there are various associated environmental risk factors including, age, stressful life trauma, diabetes, gender and others that contribute to determining whether an individual is at risk for AD (Herrup, 2010; Traynor et al., 2010; Placanica et al., 2009).

AD is characterized by the deposition of aggregated amyloid-β (Aβ) peptides in the form of extracellular senile or neuritic plaques and hyperphosphorylated tau protein in the form of intracellular neurofibrillary tangles (NFTs) (Bertram et al., 2010). The emerging amyloid hypothesis for the aetiology of AD has become fairly inclusive in the recent years. The newer thoughts continue to account for the basic chemistry of AD aetiology underlined by the *amyloid cascade hypothesis*; however networks of

interaction have emerged dictated by the biology of AD aetiology (Herrup, 2010).

Amyloid Cascade Hypothesis - As traditionally described, the amyloid cascade hypothesis is initiated in the cases of FAD where the amyloid precursor protein (APP) is aberrantly cleaved due to mutations within its gene or the genes of PSEN1 and PSEN2, constituents of γ-secretase protease complex responsible for cleaving APP to smaller Aβ peptides (Tanzi et al., 2005). APP is an integral membrane protein that has a large extracellular amino-terminal domain and a small intracellular cytoplasmic domain (De Strooper and Annaert, 2000). It is ubiquitously expressed in many tissues, however in the central nervous system it is localized to neurons, with highest concentration present at postsynaptic densities, axons and dendrites (Schubert et al., 1991; Priller et al., 2006; Zheng and Koo, 2006). The primary function of APP is not clear however studies show that APP likely regulates synapse formation and contributes to neural plasticity (Schubert et al., 1991; Turner et al., 2003). As studies indicate, there is continuous APP production and axonal transportation to both peripheral and central synapses even in adulthood, suggesting that perhaps APP is playing continuous roles in regulating pre-synaptic structure and function (Sisodia et al., 1993). In addition, APP null mutant mice show reductions in synaptic transmission, locomotor activity, body weight, and grip strength evidence of sensorimotor in addition to memory deficits (Zheng et al., 1995).

APP is processed and cleaved by three protease families: α-secretases, β-

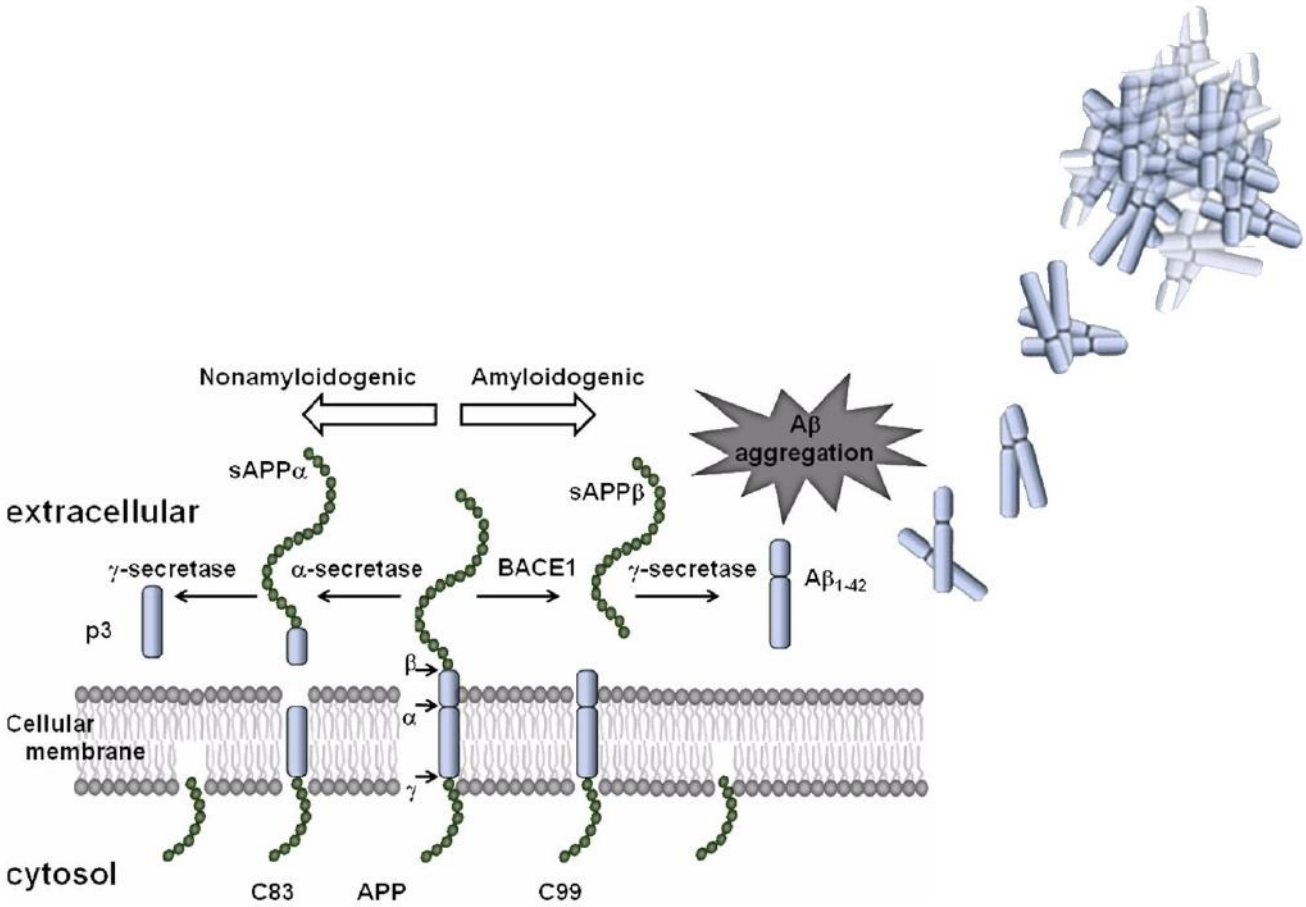

Figure 6. APP Processing via the Proteases α-, β-, and γ- Secretases and Aβ Accumulation.A schematic diagram representing APP processing in non amyloidogenic and amyloidogenic pathways. In the non-amyloidogenic pathway, the α-secretase generates sAPPα and C83. In the amyloidogenic pathway, the β- secretase generates sAPP β and C99. C99 is a substrate for γ-secretase which generates the Aβ peptide. Aβ peptides aggregate into multimers and subsequently forms the Aβ plaque. (This figure is adapted from Lee et al., 2010).

secretases, and γ-secretases. Cleavage by α- and β-secretases leads to removal of amino-terminal fragment known as soluble APP (sAPP) (Figure 6). Alternatively, APP is processed to produce Aβ peptide via sequential cleavage mediated initially by the β-secretase BACE1 followed by γ-secretases as shown in Figure 6 (Tanzi et al., 2005). Aberrant processing of mutated APP leads to the production of excess 42 amino acid (aa) form of Aβ peptide ($A\beta_{42}$). Initially alpha-helical in conformation, due to the large number of hydrophobic amino acids, $A\beta_{42}$ has a high tendency to adopt a β-sheet secondary structure, which in the presence of metal ions can oligomerize to form toxic oligomers (Jarrett et al., 1993; Walsh et al., 2000). These oligomers, in turn, aggregate to form proto-fibrils, which are also very toxic and themselves aggregate together to form fibrils. Numerous fibrils stick together and construct Aβ plaques (Walsh et al., 1999). According to the amyloid cascade hypothesis, this sequential processing of APP to $A\beta_{42}$ monomers, oligomers, proto-fibril, fibrils, and Aβ plaques plays a role in neuronal dysfunction and dementia in AD; although it is suggested that the plaques themselves are repositories for the more toxic intermediate assemblies (oligomers and protofibrils) of Aβ (Finder and Glockshuber, 2007).

Lipid Metabolism in AD - APP processing is regulated in part, by lipid homeostasis, linking AD pathogenesis to lipid metabolism (Grösgen et al., 2010). A large body of research is emerging to suggest that Aβ oligomers destabilize plasma membrane, as evident in rapid and reversible calcium leakage induced by exposure to Aβ, and that this mechanism represents a primary defects in AD (Florent-Béchard et al., 2009). Moreover, it has been shown that disrupted lipid metabolism may lead to

destabilization of amyloid fibrils that can easily revert to soluble and highly toxic Aβ aggregates (Martins et al., 2008). Klunk *et al.* showed that membrane phospholipid metabolites, including glycerophosphocholine, glycerophosphoethanolamine, and aglycerophosphate, promote the aggregation of Aβ (Nitsch et al., 1992; Klunk et al., 1996; Klunk et al., 1997). Sweet *et al.* and our laboratory have shown that glycerophosphocholine metabolites increase in AD brain and are associated with enhanced psychosis (Sweet et al., 2002; Ryan et al., 2009). Also, an increase in free fatty acid levels observed in early stage AD has been associated with early AD inflammatory processes, suggesting the likelihood that calcium dependent phospholipases may play a crucial role in generating lipid second messengers involved in adverse cascades (Florent-Béchard et al., 2009; Sastre et al., 2006). In regard of this for example, our lab has shown that levels of PAF increase in human Alzheimer Disease brain and in 4-month-old TgCRND8, mouse model of AD (Ryan et al., 2009).

Microglial Activation in AD - Microglia are one type of the three glial cells present in the central nervous system (CNS). Surrounded by capillary epithelial cells that form the blood-brain barrier (BBB), microglia are ubiquitously distributed in the CNS, making up about 20% of the total glial cell population in the brain (Ling et al., 1993; Nakamura, 2002). Activated microglia play the classic role as "scavengers" for the maintenance of the CNS (Ling et al., 1993). The primary roles of microglia in the CNS consist of distinct immune function and rapid response to injury- allowing them to maintain a healthy neuronal environment (Nakamura, 2002). Microglia

continuously scan the CNS for damaged neurons, plaques, and infectious agents and play an important role in re-establishing a functional environment in CNS by entering damaged regions and clearing the cellular debris left behind by dying cells (Nakamura, 2002; Ling et al., 1993).

There are two types of microglia; the resident microglia (ramified) and the newly differentiated microglia that derive from the bone marrow stem cells (Gehrmann et al., 1995; Simard and Rivest, 2006). Resident microglia rapidly transform from a quiescent state to an activated state (amoeboid) in response to brain injury (Gehrmann et al., 1995). Even though greater portion of resident microglia exist in the CNS since the early stages of development, studies indicate that bone marrow stem cells can penetrate the CNS and give rise to new microglia (Simard and Rivest, 2006; Iwata et al., 2001).

Activation of microglia consists of proliferation, a change in morphology into an amoeboid shape, and the phagocytosis of damaged cells (Ling and Wong, 1993). Microglial cells play a central role in mediating inflammatory processes in the CNS that are associated with neurodegenerative diseases such as AD (Ling and Wong, 1993). Aβ plaques in AD attract activated microglia-both residential and bone marrow derived (Figure 7) (Simard and Rivest, 2006). Activated microglia can partially eliminate Aβ plaques through cell-specific phagocytosis and are controlled by stimulation of microglia with cytokines (IL-1β, IL-6, TNFα, and etc.) chemokines, and

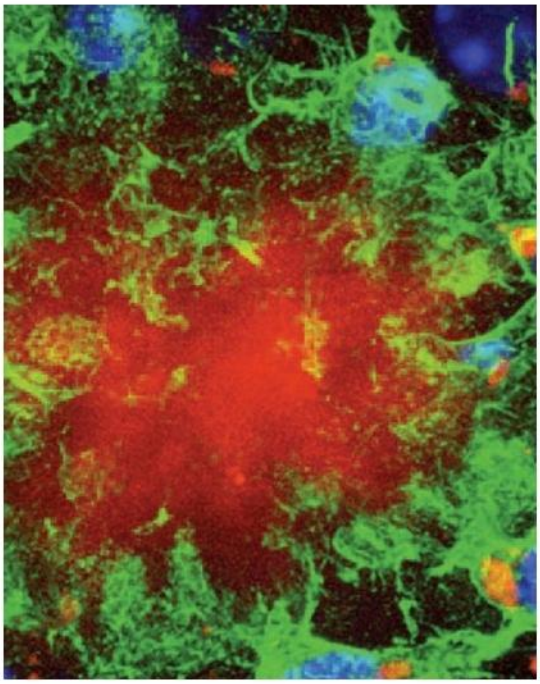

Figure 7. Activated Microglia Surrounding Aβ Plaques. Activated microglia are depicted in green surrounding Aβ plaque in red. Blue represents nuclear marker. (This figure was reproduced from Simard and Rivest, 2006.)

lipid autacoids such as PAF (Selkoe, 2001; Nakamura, 2002; Simard and Rivest, 2006; Nakamura, 2002). Furthermore, it has been shown that degradation of Aβ by microglia is carried out principally by Aβ degrading enzymes such as neprilysin and related proteases (Iwata et al., 2001; Spencer et al., 2008). Neprilysin has been implicated as a major Aβ degrading enzyme in the brain, and it plays a key role in Aβ degradation-accumulation equilibrium in AD (Tanzi et al., 2004; Spencer et al., 2008).

Rationale and Hypothesis- Our lab has shown that levels of PAF increase in human AD brain and in 4 month old TgCRND8 mouse model of AD (Ryan et al., 2009). As previously described, PAF binds a single G-protein coupled receptor (PAFR) (Honda et al., 2002). In rats, PAFR is expressed at high levels by microglia and at lower levels by neurons, notably pyramidal neurons in the hippocampus (Mori et al., 1996; Bennett et al., 1998; Aihara et al., 2000). Neuronal expression has been shown to facilitate long-term potentiation in *ex vivo* cultures of rat cortex, hippocampus, and medial vestibular nucleus (Wieraszko et al., 1993; Kato et al., 1994; Pettorossi and Grassi, 2001; Kondratskaya et al., 2004; Heusler and Boehmer, 2007; Saraf et al., 2003).

In primary rat hippocampal cultures, PAF can alter quantal release of glutamate as well as modulate L-3-methylglutamic acid (mGlu), N-Methyl-D-aspartate receptor (NMDAR), and GluR1 activity, in part, through the downstream activation of calcium/calmodulin-dependent protein kinase II (Moriguchi et al., 2010). *In vivo,* hippocampal administration of PAFR antagonist impair behavioural indices of spatial learning and memory and induces retrograde amnesia whereas direct application of non-metabolizable PAF analogs enhances hippocampal learning in rats (Teather et al., 1998; Saraf et al., 2003). These data suggest that activation of *neuronal* PAFR by PAF in Alzheimer Disease will improve or at least maintain hippocampal-dependent indices of learning and memory. *I argue, however, that these effects are cell-specific.* For example, the activation of *microglial* PAFR by PAF elicits a powerful chemotactic response (Pettorossi et al., 2001). Also, activated microglia in hippocampus is associated with the attenuation of LTP and impairment of spatial

learning and memory (Min et al., 2009). Acute microglial accumulation is associated with the clearance of Aβ oligomers and plaques through synthesis and release of the Aβ degrading enzyme neprilysin (Hickman et al., 2008). Chronic accumulation, however, is associated with a decrease in neprilysin expression (Hickman et al., 2008). Moreover, while PAFR is likely expressed by CA1 neurons in rat hippocampus, this may not be the case in mice. CA1 LTP is not impaired in PAFR KO mice, although deficits have been reported in the dentate gyrus (Kobayashi et al., 1999; Chen et al., 2001). Thus, a better understanding of the cellular distribution of PAFR is essential for interpreting the underlying mechanisms of PAF-mediated effects in AD and related experimental models. **I therefore hypothesize that PAFR expression in mouse hippocampus underlies reported differences in PAF-mediated effects on learning and memory in mice and rats.** To test this hypothesis, I propose first to localize PAFR mRNA in murine hippocampus and then assess the impact of PAFR null mutation on hippocampal AD pathology and function using the TgCRND8 mouse model. Following this analysis, I crossed PAFR KO mice onto the TgCRND8 mouse model of AD and assessed the impact on (a) learning and memory in WT mice and (b) plaque size and number in transgenic mice/Alzheimer disease. These objectives were achieved in three specific aims: (1) To localize PAFR mRNA in mouse hippocampus by *in situ* hybridization. (2) Using a loss of function approach, assess role of PAFR in hippocampal-dependent indices of learning and memory in mouse. (3) Using a loss of function approach, determine whether loss of PAFR from microglia alters amyloid-beta plaque accumulation in a transgenic mouse model of AD.

Chapter 2

MATERIALS AND METHODS

Breeding pairs of PAFR KO mice in a hybrid C57BL/6J x 129/Ol background (Ishii et al., 1998) were the kind gift of Dr. Takao Shimizu (University of Tokyo, Japan) and were back-bred for 15 generations into a C57BL/6 lineage in the Bennett laboratory. Breeding pairs of TgCRND8 mice, expressing a double mutant (KM670/671NL+V717F) form of the human amyloid precursor protein under the control of the prion cos-tet promoter (Chishti et al., 2001) were kindly provided by Dr. Paul Fraser (University of Toronto, Ontario). When crossed with PAFR KO mice, progeny (NonTg PAFR WT, NonTg PAFR KO, Tg PAFR WT, and Tg PAFR KO) were a mixed hybrid of C3H and C57BL/6 backbred for 4 generations to a C57BL/6 background.

1. **Generation of PAFR WT Riboprobe**

1.1. *Animals* -C57BL/6 wild-type (PAFR WT) and N15 PAFR KO mice at 4 months of age were euthanized by lethal intraperitoneal (IP)injection with sodium pentobarbital. All procedures were in accordance with the Animal Care Committee of the University of Ottawa following the guidelines set forth by the Canadian Council on Animal Care.

***1.2**. Genotyping* - Polymerase Chain Reaction (PCR) was performed to identify or confirm the genotypes of all mice. DNA was isolated from 2-5 mm tail biopsy. Tails were incubated for digestion overnight in 100 mM Tris-Cl (pH8.5), 5 mM EDTA, 200 mM NaCl, 0.2% SDS, and 10 μg/ml proteinase K solution at 55°C. Once tails were digested overnight, phenol/chloroform/isoamyl alcohol (25:24:1) was added and the samples were spun for 10 min at 12,000 g. DNA was then collected from the supernatant, precipitated with isopropanol, and spun for another 10 min at 12,000 g. Samples exhibited pellets of DNA at the bottom of the tubes which were washed with 70% ethanol and left to dry at room temperature. Once the ethanol was evaporated, DNA was re-suspended in 10 mM Tris-Cl (pH 7.5) and 1 mM EDTA (pH8.0) solution in double distilled water (ddH_2O). The DNA in solution was used to genotype for *PTAFR* or *neomycin* genes. Primer sequences are provided in Table 1.

Once DNA was isolated from individual mice, PCR reactions were conducted using primer sets respective to the genes of interest (Table 1). Although distinct primer sets were used to genotype for PAFR WT and KO mice, a common master mix (MM) solution was used for both. The MM per one reaction consisted of: 16 μL of Nuclease-Free H_2O (NF-H_2O), 2.5 μL of 10X Advantage2 PCR Buffer (Clontech), 0.25 μL of 10 mM deoxyribonucleotide triphosphates (dNTPs), 0.5 μL of 0.2 μg/μL forward primer (IDT), 0.5 μL of 0.2 μg/μL reverse primer (IDT), and 0.25 μL of 50X Advantage2 DNA Polymerase Mix (Clontech). For every PCR reaction, 5 μL of DNA was added to 20 μL of MM and ran through a Whatman Biometra T-Gradient thermocycler (Montreal-Biotech Inc., Kirkland, QC, Canada). The PCR cycling parameters for both PAFR WT and

Table 1.Primer Sequences for PCR Reactions.

Gene	Primer	Sequence
PAFR WT	Forward	*5′ TAT GGC TGA CCT GCT CTT CCT GAT 3′*
	Reverse	*5′ TAT TGG GCA CTA GGT TGG TGG AGT 3′*
PAFR KO	Forward	*5′ GCC TGC TTG CCG AAT ATC ATG GTG GAA AAT 3′*
	Reverse	*5′ GCG ATG CGC TGC GAA TCG GGA GCG ATA 3′*
GAPDH	Forward	*5′ TGG TGC TGA GTA TGT CGT GGA GT 3′*
	Reverse	*5′ AGT CTT CTG AGT GGC AGT GAT GG 3′*
Tg	DW191	*5′ GGC CGC GGA GAA ATG AAG AAA CGC CAA GCG CCG TGA CT 3′*
	DW229	*5′ TGT CCA AGA TGC AGC AGA ACG GCT ACG AAA A 3′*

PAFR KO are as follows: 95°C for 10 min, 30 cycles (PAFR WT) and 35 cycles (PAFR KO) of [95°C for 20 sec, 65°C for 20 sec, 70°C for 50 sec], and finally held at 4ºC.

1.3. *Tissue Preparation and Total RNA Isolation* - Total RNA was extracted from cerebrum, cerebellum, heart and lung tissues dissected from anaesthetized and decapitated PAFR WT and KO mice. Tissues were homogenized in 1 mL Trizol reagent (Invitrogen) per 50-100 mg of tissue. Homogenized samples were incubated for 5 min at room temperature, at which point 200 µL of chloroform per 1 mL of Trizol was added. Samples were gently mixed for 15 sec and spun at 12,000 g for 15 min at 4ºC. The aqueous phase containing total RNA was removed and placed into a new eppendorf tube. Subsequently, 500 µL of isopropanol per 1 mL of Trizol was added to precipitate total RNA. The solution was then incubated for 10 min at room temperature and then spun at 12,000 g for 10 min at 4ºC. Upon centrifugation, pellets were evident at the bottom of the tubes which were washed with 1 mL of 75% ethanol per 1 mL of Trizol. Ethanol was discarded and the pellets were air dried for about 10 min and re-suspended in 30 µL of NF-H_2O. Unless otherwise indicated, all materials were obtained from Fisher Scientific.

Total RNA was also extracted from PC12 cells which were obtained from four confluent 10 cm^2 dishes. Dishes containing confluent cells were kept on ice as they were washed twice with 10 mM sterile PBS (10 mM sodium phosphate and 154 mM NaCl). Homogenized cells were pooled from all four confluent dishes as 1 mL of

Trizol reagent was used for all four dishes. Once cells were homogenized and pooled together, the subsequent total RNA extraction procedures followed closely to that described above for total RNA extraction from tissues. Unless otherwise indicated, all materials are obtained from Fisher Scientific.

1.4. *Reverse Transcription Polymerase Chain Reaction (RT-PCR)* - Total RNA was isolated from PAFR WT and PAFR KO mouse cerebrum, cerebellum, heart, and lung tissues as well as from PC12 cells using Trizol Reagent (Invitrogen) as described above. In order to degrade any genomic DNA contamination in these samples the total RNA was DNAse treated. DNAse treatment mixture consisted of 4 µg of total RNA, 1 µL of RQ1 RNase-free DNAse, 1 µL of 10X Buffer (Promega, Madison, WI, USA) and *X* µL of NF-H_2O for a total volume of 10 µL. DNAse treated mixtures were gently added and mixed and were then incubated for 30 min at 37ºC. Following incubation, 40 µL of NF-H_2O and 50 µL of phenol/chloroform/isoamyl alcohol (25:24:1) were added to the samples for a final volume of 100 µL. The samples were then vigorously vortexed and centrifuged at maximum speed for 1 min. The upper aqueous phase was transferred to a new tube where 5 µL of 3 M sodium acetate and 200 µL of 100% ethanol were added. Samples were inverted twice and left at -80ºC overnight.

The following day, DNAse treated RNA samples were dissolved as follows. Samples were centrifuged at maximum speed for 10 min at 4ºC. The supernatant was discarded and the pellet containing RNA was washed twice with 70% ethanol in

Diethylpyrocarbonate (DEPC) (Sigma) water (DEPC-ethanol), inverted twice, and centrifuged at maximum speed for 1 min. RNA pellets were air dried for about 10 min and re-suspended in 10 µL NF-H_2O, where they were ready for reverse-transcription.

Two sets of reactions were performed for each sample; one where 50 units of Superscript II Reverse Transcriptase (RT) was added and one where it was not added, denoted as positive-RT (+ RT) and negative-RT (- RT) respectively. Also, first-strand synthesis was performed using pdN6 (Promega) random primers. Thus, in the + TR reaction set, the following were added: 5 µL (2 µg) of DNAse-treated RNA, 6 µL of NF-H_2O, and 1 µL of 0.5 µg/ µL pdN6 random primers per reaction. In the - TR reaction set the following were added: 5 µL (2 µg) of DNAse-treated RNA, 7 µL of NF-H_2O per reaction, and 1 µL of 0.5 µg/ µL pdN6 random primers per reaction. Both reaction sets were incubated at 70ºC for 10 min, and then incubated at 4ºC for 2 min using a Whatman Biometra T-Gradient thermocycler (Montreal- Biotech Inc., Kirkland, QC, Canada). Once samples were incubated at 4ºC, the following were added per reaction to both sets: 4 µL of 10X 1st strand buffer, 2 µL of 0.1M dithiothreitol (DTT), and 1 µL of 10 mM dNTPs. Both reactions were incubated at 37ºC for 2 min before pausing to add 1 µL (50 units) of Superscript II RT to the + RT reaction set. Incubated all samples successively at 25°C for 10 min; 42°C for 60 min; 50°C for 30 min; and held at 4°C. All reagents were obtained from BD Biosciences, San Jose, CA, USA unless otherwise indicated.

Random primed cDNA was used to conduct PCR reactions for GAPDH and PAFR WT. PCR reaction was performed using primer sets specific for GAPDH for all samples in both the +RT and -RT reactions. The MM per one reaction consisted of: 36 μL of NF-H_2O, 5 μL of 10X Advantage2 PCR Buffer (Clontech), 4 μL of 10 dNTPs, 1 μL of 10 pmol/μL GAPDH forward primer (IDT), 1 μL of 10 pmol/μL GAPDH reverse primer (IDT), and 1 μL of 50X Advantage2 DNA Polymerase Mix (Clontech). For every PCR reaction, 2 μL of cDNA was added to 48 μL of MM and ran through a Whatman Biometra T-Gradient thermocycler (Montreal-Biotech Inc., Kirkland, QC, Canada). The PCR cycling parameters for GAPDH include: 105 °C lid temperature, 35 cycles of [94ºC 5 min, 59°C for 25 sec, 72°C for 1 min], 72°C for 7 min, and finally held at 4ºC.

The pool of cDNA was also used to amplify the 311 base pairs generated using PAFR WT forward and reverse primers (Table 1). The MM per one reaction consisted of: 16 μL of NF-H_2O, 2.5 μL of 10X Advantage2 PCR Buffer (Clontech), 0.25 μL of 10 mM dNTPs, 0.5 μL of 0.2 μg/μL PAFR WT forward primer (IDT), 0.5 μL of 0.2 μg/μL PAFR WT reverse primer (IDT), and 0.25 μL of 50X Advantage2 DNA Polymerase Mix (Clontech). For every PCR reaction, 5 μL of cDNA was added to 20 μL of MM and ran through a Whatman Biometra T-Gradient thermocycler (Montreal- Biotech Inc., Kirkland, QC, Canada). The PCR cycling parameters for PAFR WT includes: 95 °C for 10 min, 30 cycles of [95°C for 20 sec, 65°C for 20 sec, 70°C for 50 sec], and finally held at 4ºC. This amplified 311 PAFR cDNA sequence was later cloned in to a pGEM-T Easy Vector and used to generate a PAFR WT riboprobe as described in the proceeding sections.

1.5. *Cloning of PAFR WT cDNA Segment* - The cloning experiment consisted of three main steps: (1) ligation of the PAFR WT cDNA insert into a pGEM-T Easy Vector, (2) transformation of competent cells, and (3) screening for transformed cells using blue white screening technique and culturing transformed cells. PAFR WT cDNA insert of 311 base pairs in length was ligated into a pGEM-T easy vector. The ligation reaction for PAFR WT cDNA insert constituted of 2X Rapid Ligation Buffer, pGEM-T Easy Vector (50ng), cDNA Product, T4 DNA Ligase (3 Weiss units/μL), and NF-H2O (Innovation). In addition, the manufacturer's positive and negative background controls were also run in this ligation reaction. The ligation reactions were mixed and incubated overnight at 4°C. The following day, transformation reaction was conducted where 50 μL of M109 High Efficiency component cells were added to 2 μL of now ligated pGEM-PAFR WT cDNA insert vector. Upon gently mixing, the transformation reactions were left on ice for 20 min. After incubation on ice, the cells were heat-shocked for 45 - 50 sec in water bath at exactly 42°C and were immediately returned to ice for an additional 2 min. Following the 2 min ice incubation, 950 μL of room temperature LB broth (with 50 mg/mL ampicillin) was added to each transformation reaction and incubated for 1.5 hr at 37°C with shaking. LB broth was prepared by mixing 1% (g/vol) tryptone, 0.5% (g/vol) yeast extract, 0.5% (g/vol) NaCl, 0.1% (g/vol) NaOH in H_2O. Subsequent to incubation, 100 μL of each transformation culture was plated on to LB/ampicillin/IPTG/X-Gal plates (detailed below) and incubated overnight at 37°C. The following day white colonies were inoculated and left to grow overnight at 37°C in LB broth (with 50 mg/mL ampicillin). Plasmid DNA was then isolated using mini prep kit as directed by the manufacturer

(QIAGEN plasmid mini kit). All reagents were obtained from Promega unless otherwise stated.

LB/Ampicillin/IPTG/X-Gal plates were made using LB-agar media and they were used for the blue white screening. The LB-agar media was prepared by mixing 1% (g/vol) tryptone, 0.5% (g/vol) yeast extract, 0.5% (g/vol) NaCl, 0.1% (g/vol) NaOH, 1.5% (g/vol) agar in H_2O. Upon thorough mixing, the LB-agar media was autoclaved and left to cool down before adding ampicillin to 50 μg/mL, X-gal (or bromo-chloro-indolyl-galactopyranoside) to 20 μg/mL, and IPTG (Isopropyl β-D-1- thiogalacto-pyranoside) to 0.1 mM. After mixing the additives, the now cooled LB- agar media was poured into petridishes of 100 mm X 20 mm forming the LB/Ampicillin/IPTG/X-Gal plates used in the cloning experiment.

1.6. *Generation of Digoxigenin Labelled Antisense Riboprobe by in vitro Transcription* - The isolated plasmid murine DNA (10 μg) was linearized using appropriate restriction enzyme. The restriction digest constituted of 10 μL of enzyme - *SalI* (200U), 10 μL of 10 X NEB Buffer 2, 1 μL of NEB BSA to a final volume of 100 μL NF-H_2O (New England Bio Labs). Restriction digests were incubated at 37^{o}C overnight. The following day linearization was verified by running a 10μl sample with the native plasmid and an appropriate DNA ladder on an (0.8%) agarose gel. After confirming that the digestion of plasmid DNA was successful, linearized DNA was purified using phenol/chloroform/isoamyl alcohol extraction. The purification of the linearized DNA was performed using the phenol/chloroform/ isoamyl alcohol

extraction. Equal volume of phenol/chloroform/isoamyl alcohol was added to the sample which was then vortexed and centrifuged at max speed for 15 sec at room temperature. Following the centrifugation, the aqueous phase was removed and pipetted into a new 1.5 mL eppendorf tube where 1/10 volume of 3 M sodium acetate (pH 5.2) and 2 - 2.5 volumes of ice cold 100% ethanol were added to the reaction mixture. The samples were incubated on dry ice for 10 min and subsequently centrifuged at max speed for 5 min. The supernatant was discarded and the remaining pellet was washed twice with 70% ethanol before letting it dry at room temperature for 10 min. The dried pellet was then re-suspended in ~30 µl of NF-H_2O, and DNA concentration was measured using a spectrophotometer. All reagents were obtained from Fisher Scientific unless otherwise indicated.

The purified linearized DNA was used in the *in vitro* transcription of digoxigenin (DIG) labelled antisense riboprobe using the Roche DIG RNA labelling kit (SP6/T7). The *in vitro* transcription reaction consisted of 1µg of linearized DNA, 10X NTP labelling mixture**,** 10X transcription buffer**,** 20 units/µl protector RNAse inhibitor, 20units/µl T7 polymerase in NF-H_2O. Mixed gently, centrifuged briefly, and incubate the samples at 37^{o}C overnight. The following day, stopped the reaction by adding 1µl of 0.5 M EDTA (DEPC-treated) pH 8.0. To purify the newly transcribed RNA riboprobe the following steps were performed. The sample was vortexed and placing in dry ice for duration of 10 min. Once the 10 min incubation in dry ice was over, the sample was centrifuged at max speed for 5 min where the supernatant was discarded. The remaining pellet was washed twice with 70% ethanol before allowing

the pellet to dry at room temperature for less than 10 min. Upon drying, the pellet was re-suspended in 100 µl of 10 mM EDTA DEPC-H_2O. The integrity of riboprobe was verified by gel electrophoresis. Electrophoresis tank was soaked in 3% H_2O_2 for 10 min and washed abundantly with dH_2O prior to use. A quantity of 3 µL of riboprobe was denatured at 70°C for 10 min, and quickly mixed with 3 µl of 6X loading buffer. Loaded the 6 µL of probe mixed with loading buffer and ran gel (1%) for 15 min at 200 V. All reagents were obtained from Fisher Scientific unless otherwise stated.

2. *In Situ* Hybridization

2.1. *Animals and Tissue Preparation* -C57BL/6 wild-type and PAFR KO mice were utilized at 4 months of age. Animals were euthanized by lethal IP injection of sodium pentobarbital and transcardially perfused with 10 mM diethylpyrocarbonate (DEPC)-PBS followed by 3.7% paraformaldehyde in 10 mM DEPC-PBS. Brains were removed and postfixed for 24 hr in this same solution, transferred to 10 mM phosphate buffer and cryosectioned (10 µm coronal and sagittal sections) using a Leica CM1900 Cryostat. All procedures were in accordance with the Animal Care Committee of the University of Ottawa following the guidelines set forth by the Canadian Council on Animal Care.

2.2. *In Situ Hybridization* - Coronal and sagittal brain sections from 4 months old PAFR WT and KO mice were utilized for *in situ* hybridization. The PAFR WT riboprobe was diluted (1:50) in pre-warmed (65ºC) hybridization buffer (10X Salt [2

M NaCl, 0.09 M Tris-HCl pH 7.5, 0.01 M Tris base, 0.05 MNaH_2PO_4*2H_2O, 0.05 M Na_2HPO_4, and 0.05 M EDTA], deionized formamide, 50% (g/vol) dextran sulphate, 10 mg/mL rRNA, and 100X Denhardt‟s). The diluted riboprobe was denatured at 70^{o}C for 10 min prior to use. Upon denaturing, 100-150 µl of the riboprobe was pipetted onto each brain slide. Slides were then covered with microscope glass slide cover slips and were placed in a humid chamber prepared from 2 sheets of 3 mm Whatman paper soaked in 50% (vol/vol) formamide/1X salt. The humid chamber containing the slides was then placed in a hybridization oven at 65^{o}C for 1 hr.

Post hybridization, slides were washed once with wash buffer (1 X SSC (sodium chloride/ sodium citrate) [3 M NaCl, 0.03 M Na_3Citrate*2H_2O pH to 7.0 with autoclaving], 50% (vol/vol) formamide, and 0.1% (vol/vol) Tween-20 all in ddH_2O) pre-warmed at 65^{o}C for 15 min. The slides were further washed twice more in wash buffer, once at 65^{o}C for 30 min and the second time at room temperature for 30 min. Following the initial three washes, the slides were incubated twice in 1 X MABT (0.5 M maleic acid, NaOH pH to 7.5, 0.75 M NaCl, and 0.5% (vol/vol) Tween-20) at room temperature for 30 min. Brain sections were then incubated with blocking solution (20% (vol/vol) Sheep serum, 2% (vol/vol) Blocking reagent (Roche), 1X MABT in ddH_2O) in a humidified chamber for 1 hr at room temperature. Upon the end of the 1 hr incubation in blocking solution, brain sections were covered with sheep anti-DIG-AP antibody (Invitrogen) diluted (1:1500) in blocking solution and incubated at 4^{o}C overnight.

Upon antibody incubation overnight, brain slides were prepared for staining reaction. As such, slides were first washed in 1 X MABT at room temperature 4 consecutive times for 10 min. The slides were then incubated twice in a pre-staining buffer (100 mM NaCl, 50 mM $MgCl_2$, 100 mM Tris pH 9.5, 0.1% (vol/vol) Tween-20 in ddH_2O) for duration of 10 min each time. Finally, the slides were incubated in a colour reaction mixture overnight in the dark at room temperature. Substrate was prepared by adding 100 mM NaCl, 100mM Tris-Cl pH 9.5, 10% (g/vol) polyvinyl alcohol in ddH_2O and heating to 85ºC. Once the polyvinyl alcohol was completely dissolved, allowed the solution to cool before adding 50 mM $MgCl_2$, 0.1% (vol/vol) Tween-20, NBT (4-Nitro blue tetrazolium chloride) (Roche) to 4.5 µl/mL, and BCIP (5-bromo-4chloro-3-indoyl-phosphate) (Roche) to 3.5 µl/mL.

The following day, the colouring reaction was stopped by washing the slides in 10 mM PBS 5 consecutive times for 10 min each. Following the washes, the slides were dehydrated as per the following consecutive steps: 2 min in ddH_2O, 2 min in 95% ethanol, 3 min in 95% ethanol, 3 min in 100% ethanol, 2 min in citrosolv, 3 min in citrosolv, and 3 min in citrosolv. Finally once they were dehydrated, the brain slides were mounted with DPX (Sigma - Aldrich) and covered with microscope glass coverslip and left to dry at room temperature. All reagents were obtained from Fisher Scientific unless otherwise stated.

3. Morris Water Maze (MWM) Analysis

3.1*. Animals* - Wild-type (n=6) and PAFR KO (n=5) littermates back-bred for only 4 generations into a C57BL/6 background were utilized at 5 month of age. We chose to test the N4 C57BL/6-CH3 hybrid line and not the N15 line as these mice were congenic to TgCRND8s (PAFR WT and KOs) used to assess plaque number as described below.

3.2. *MWM* - The most widely used paradigm for evaluating learning and memory in rodents is the Morris water maze (MWM) experiment (Morris, 1984). MWM entails a round pool that is filled with water. A platform is placed at a fixed location in the pool where it is hidden, as the water is made opaque by white paint. In this experiment, two visual cues were placed at two places for the entire duration of the experiment; one black "X" at the Front wall, and a filled square at the Left wall. The idea behind this assessment is that the animals must learn to find this hidden platform using visual cues and repeated trials. The principle behind this task lies in the fact that rodents are adverse to water and are highly motivated to escape from the water. As such, the animals learn and remember where the platform is to escape from the water quickly. They can enter the pool from four different starting points, Right, Left, Back, and Front in respect to the position of the mouse in the room (Figure 8). The mice are given a number of training days where in each day they enter the pool four times, corresponding to the four entrance positions. Ideally, upon a number of trials the animals should learn to locate where the platform is. The strength of learning is assessed later (immediate day after training days) by a probe trial. At the probe trial, the hidden platform is removed and the position of animals and time spent by

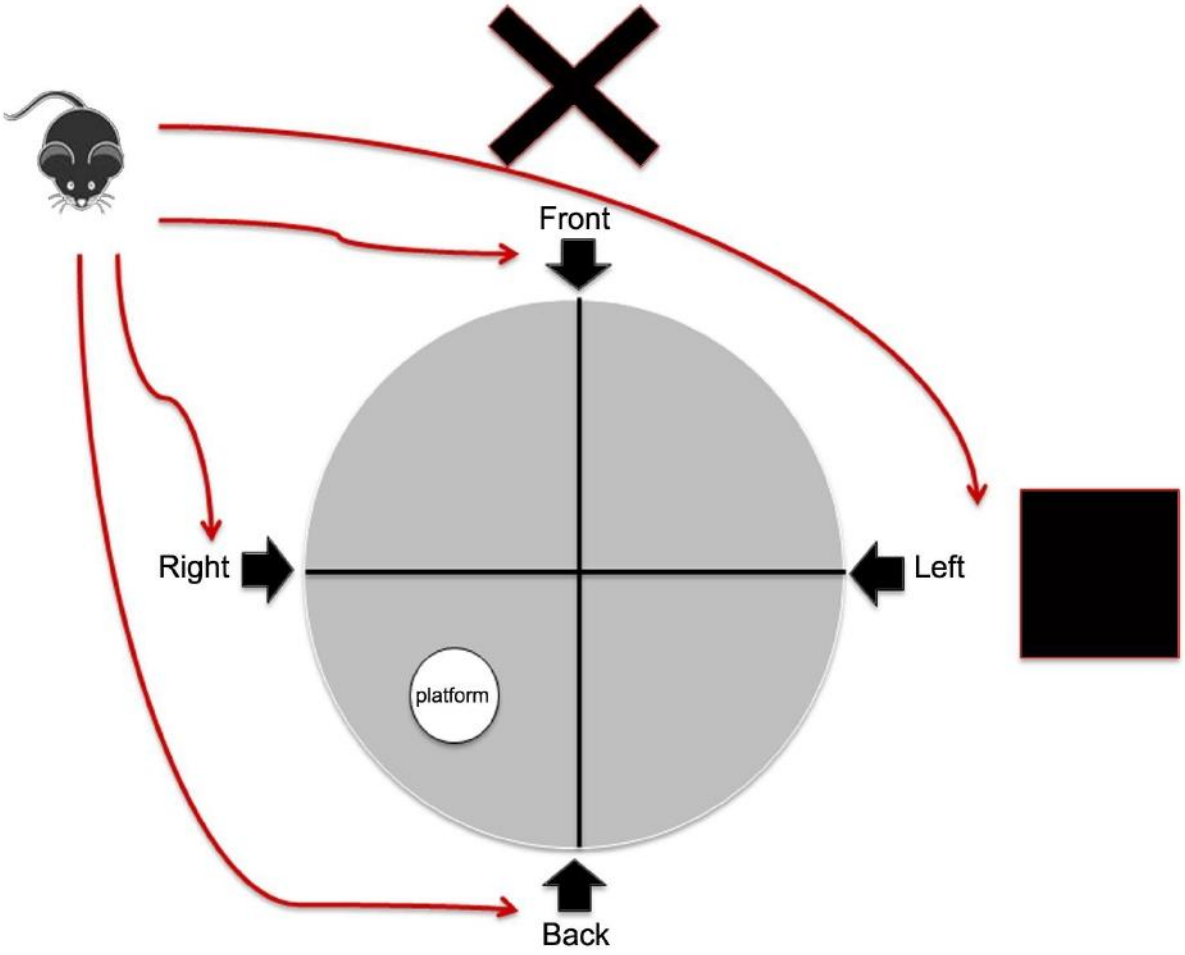

Figure 8. Morris Water Maze (MWM) Arena. The Morris water maze (MWM) arena is a circular pool filled with opaque water. There are four portals in which mice may enter the pool, Right, Back, Left, and Front in respect to mouse position (black mouse). The hidden platform is located in the Right Back zone. There are two visual cues as indicated by the "X" and filled square, both in black.

animals looking for the platform is measured and recorded by a camera connected to a computer (Morris, 1984). In this particular MWM analysis, PAFR WT and KO mice were trained for eight consecutive days, where each day they were given four trials with randomized order of entrance. Upon the probe trial on the 9th day, the platform was removed and mice were arbitrarily entered the pool from one of the four entrances and left to swim for 60 seconds.

3.3. *Data Analysis* - The parameters that are analyzed in this experiment include average distance moved, average velocity of mice, average time spent in platform zone, average latency to find the platform, average escape latency upon Probe trial, and lastly average thigmotaxis experienced by mice. In must be noted however that for all parameters except average escape latency upon Probe trial, the average is taken from all four trials conducted on each of the eight training days.

3.4. *Statistical Analysis* - Student"s *t*-test (unpaired) was performed to assess the significance of the data collected from average distance moved, average velocity of mice, average time spent in platform zone, average escape latency upon Probe trial, and average thigmotaxis of mice. A two-way analysis of variance (ANOVA) was performed to assess the significance of the data collected from average escape latency.

4. Amyloid β Analysis in TgCRND8 Mice

4.1. *Animals* - TgCRND8 mice were bred with N15 PAFR KO mice. The heterozygote offspring were then bred with each other to generate the four congenic littermates that were used in this study; TgPAFR KO, TgPAFR WT, NonTgPAFR KO, and NonTgPAFR WT. All animals were N4 generation (C57BL/6) and were sacrificed at 4 months, 6 months, and 8 months of age. Animals were euthanized by lethal IP injection with sodium pentobarbital and transcardially perfused with 10 mM PBS followed by 3.7% paraformaldehyde in 10 mM PBS. Brains were removed and postfixed for 24 hr in this same solution and transferred to 10 mM phosphate buffer and cryosectioned (10 μm coronal sections) using a Leica CM1900 Cryostat. Animal numbers for 4, 6, and 8 months of age respectively include: TgPAFR WT n of 4, 6, and 4; TgPAFR KO n of 3, 8, and 6; NonTgPAFR WT n of 2, 2, and 1; and NonTgPAFR KO n of 4, 3, and 4. All procedures were in accordance with the Animal Care Committee of the University of Ottawa following the guidelines set forth by the Canadian Council on Animal Care.

4.2. *Genotyping* - PCR for PAFR WT and KO was performed as explained in section 1.2.The master mix for Tg genotyping consisted of: 14 μL Nuclease-Free H_2O, 2.5 μL 10X Advantage2 PCR Buffer (Clontech), 0.5 μL dNTPs (10 mM), 2 μL DW191 primer (10 pmol/μL, IDT), 2 μL DW229 primer (10 pmol/μL, IDT), and 0.5 μL 50X Advantage2 DNA Polymerase Mix (Clontech). For every PCR reaction, 5 μL of DNA was added to 20 μL of MM and ran through a Whatman Biometra T-Gradient thermocycler (Montreal-Biotech Inc., Kirkland, QC, Canada). The PCR cycling parameters include: 94 °C for 3 min,

35 cycles of [94 °C for 20 sec, 68 °C for 20 sec, and 72°C for 90 sec], 72°C for 7 min, and finally held at 4ºC. Primer sequences are provided in Table 1.

4.3. *Immunohistochemistry* - Sections were washed in 10 mM PBS (pH 7.0) for 30 minutes and incubated overnight with primary antibody, mouse anti-4G8 diluted (1:500, Signet) in 3% (vol/vol) bovine serum albumin + 0.3% (vol/vol) Triton X-100 in PBS. Mouse anit-4G8 recognizes both murine and human Amyloid β (Signet). After the primary antibody incubation, brain sections were washed twice more with PBS for 15 minutes each and incubated for an hour in secondary antibody, FITC-labelled anti-mouse IgG diluted (1:1000, Signet) in 3% (vol/vol) bovine serum albumin +0.3% (vol/vol) Triton X-100 in PBS. Following the secondary antibody incubation, more washing steps were performed (three times for 10 min), where subsequently sections were mounted with 0.05% p-phenylenediamine in PBS/glycerol (pH 8.0) and covered with microscope glass cover slips. All reagents were from Fisher Scientific unless otherwise indicated.

4.4. *Data Analysis* - Four brain regions were examined including: the anterior cortex (AC) and the basal forebrain (BF) at the anterior of the brain and the posterior cortex (PC) and the hippocampus (H) at the posterior of the brain. The positions of the photomicrographs taken (10X magnification) are defined in Figure 9, where they collectively scan all regions under investigation. Immunofluorescence was detected using a Leica DMXRA2 epifluorescence microscope where anti-4G8-reactive plaques were quantified using Openlab software v5.05 (Improvision, Lexington, MA,

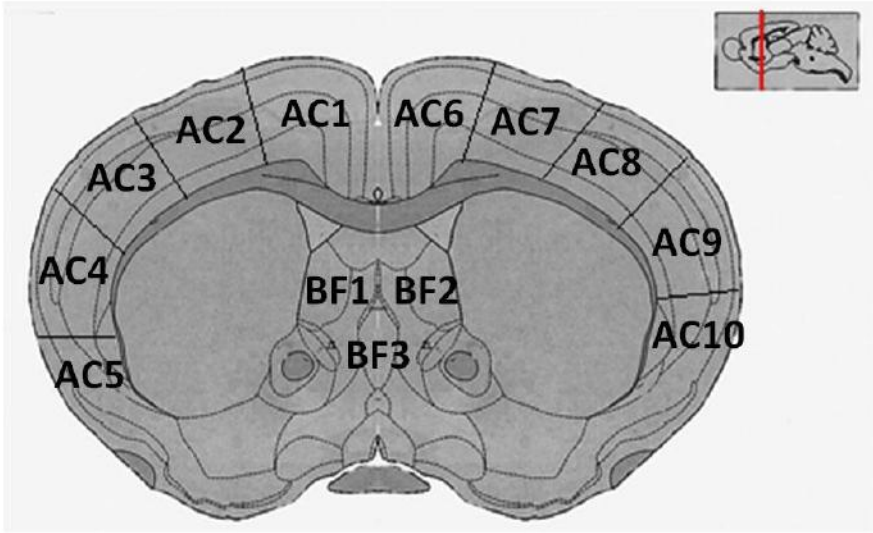

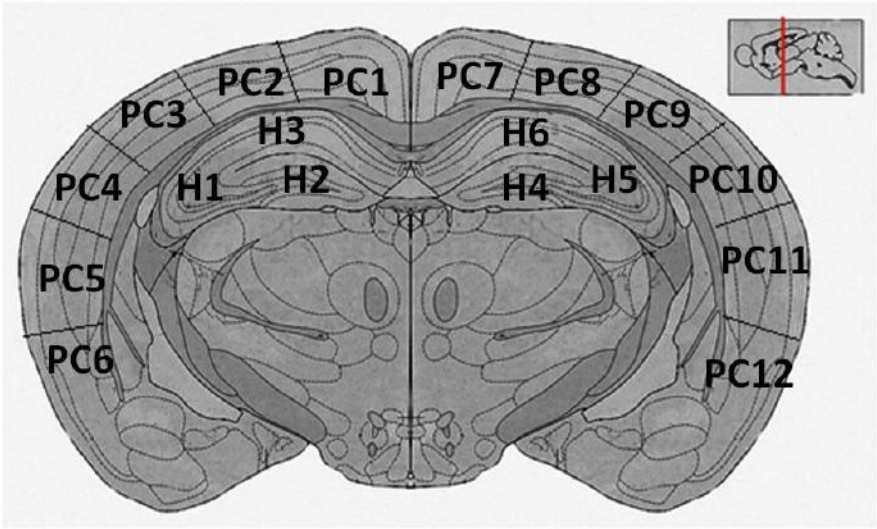

Figure 9. Brain Regions Analyzed in Aim 2 and Position of Photomicrographs. A, Ten fields of the anterior cortex were analyzed (AC1-AC10) and three fields of the basal forebrain (BF1-BF3) in the anterior of the brain. All sections were between bregma 0.90 mm and 0.50 mm. B, Twelve field encompassing the posterior cortex (PC1-PC12) and six fields encompassing the hippocampus (H1-H6) were analyzed. Diagrams represent coronal sections; insets depict the sagittal position of these sections. All sections were between bregma -1.30 mm and -2.40 mm.

USA). Plaques were defined as immunoreactive compacted and spherical aggregates. The number of plaques was determined in each field and total number of plaques summed across all fields to obtain a single measure per animal per region. The area of each region of interest was determined from each field and data are expressed as (plaque counts/ 1 mm^2).

4.5*. Statistical Analysis* - A two-way analysis of variance (ANOVA) was performed to assess the significance of the data followed by *post-hoc* Tukey tests, to identify significant differences between groups, i.e., comparing TgPAFR KO to TgPAFR WT at the different age groups.

Chapter 3

RESULTS

Aim 1 - Localize PAFR mRNA in mouse hippocampus by *in situ* hybridization.

PAFR WT Riboprobe - The objective of this aim was to localize PAFR mRNA expression in murine hippocampus by *in situ* hybridization. To reach this goal, a probe was designed to hybridize to the region that is disrupted in PAFR KO mice within the PAFR open reading frame (ORF). As described previously, all of PAFR coding sequence is within a single exon which was disrupter with a PGK-neomycin cassette in the PAFR KO mice (Ishii et al., 1998). Consequently, my probe recognizes 311 bases that cover exactly 127 bases upstream and 184 bases downstream of the site where PGK - neomycin cassette was inserted in the *PTAFR* gene (Figure 10A and B).

RT-PCR was performed targeting this specific amplicon. Indeed, as indicated by RT-PCR analysis the cDNA of this 311 stretch of RNA was evident in PAFR WT brain, lung and heart, whereas it was absent in the same tissues of PAFR KO mice (Figure 10C). GAPDH amplification was performed to confirm template integrity; all samples exhibited a GAPDH cDNA fragment. Along with the RT-PCR reactions, duplicate samples were run where the enzyme reverse transcriptase was not included (-RT). There were no cDNA fragments evident in the-RT samples. Furthermore, there was a definite band in the PCR reaction positive control (PAFR WT genomic DNA),

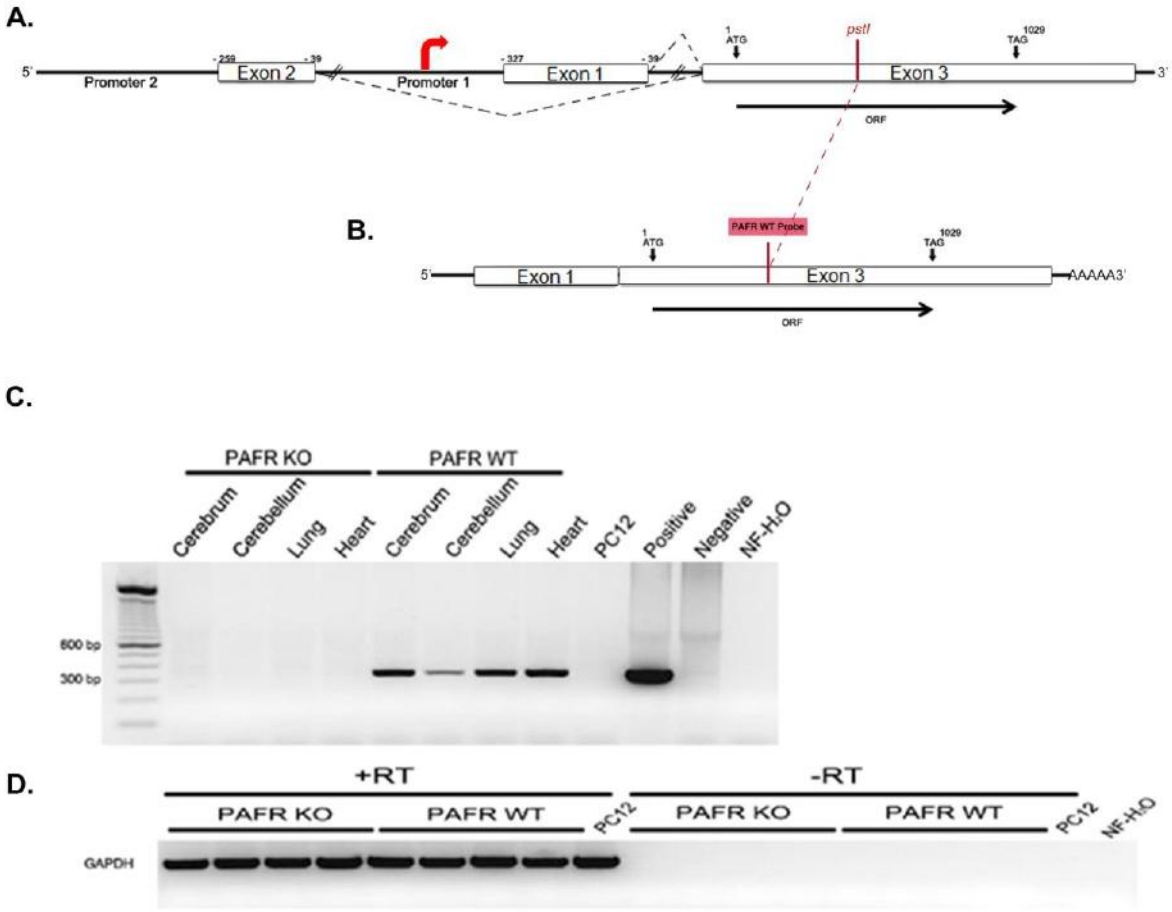

Figure 10. PAFR WT Probe Design.A, illustrates the *PAFR* gene. The three exons of *PAFR* gene are depicted, where the entire open reading frame lies in exon three. The restriction site for*PstI* is indicated as this was the site where the *PAFR* gene was disrupted by a PGK - neomycin cassette. Red arrow indicates transcription initiation of PAFR Transcript 1 as shown in B (Modified from Ishii and Shimizu, 2000). B, schematic diagram of PAFR Transcript 1, illustrating the WT mRNA sequence (311 bases) amplified by RT-PCR and cloned as cDNA into pGEM T-Easy vector for *in vitro* transcription of a DIG-labelled riboprobe. Note that the red line indicates the location where PGK-neomycin cassette was inserted in *PAFR* gene. C, RT-PCR of samples prepared from PAFR WT and PAFR KO tissue and PAFR negative PC12 cells using the primers optimized to generate the riboprobe amplicon. As the primers amplify product on a single exon, the positive and negative controls to establish reaction efficiency were genomic DNA from PAFR WT and PAFR KO mice respectively. Reactions processed in the absence of template (NF - H_20) were used to confirm lack of genomic DNA contamination in the reaction mixture. D, to confirm both template integrity and lack of genomic contamination, samples were subjected to reverse transcription in the presence (+RT) or absence (-RT) of reverse transcriptase and processed for either PAFR (data not shown) or GAPDH. Note that all samples contain template and none are contaminated with genomic DNA.

whereas it was absent in the negative control (PAFR KO genomic DNA). Lastly, the lane of NF-H_2O exhibited no bands. As such, the cDNA of the 311 bp PAFR WT fragment was ligated into pGEM T-Easy vector flanked by T7 (reverse) and Sp6 (forward) promoters. The pGEM T-PAFR WT vector was cloned and subsequently sequenced (Figure 11, The Sprott Center for Stem Cell Research, University of Ottawa, Ottawa, ON). Sequencing of selected colonies showed that the 311 bp PAFR WT insert was successfully cloned, as evident by sequence alignment.

In Situ Hybridization - *In situ* hybridization was performed using this DIG labelled PAFR WT riboprobe on cryosectioned coronal and sagittal brain slices of murine PAFR WT and PAFR KO controls. There appears to be an intense signal in PAFR WT mouse hippocampus tissue at the 5X magnification (Figure 12C). This signal is absent in tissue of PAFR KO mouse in the same magnification (Figure 12D). Indeed, as evident in the 40X magnifications, the signal appears further definite in the CA1 and CA3 regions of the PAFR WT hippocampus. Conversely, there appears to be no intense signal evident in the corresponding PAFR KO hippocampus regions in the same magnification. Further magnifications of the signals in the PAFR WT CA1 and CA3 appear to exhibit small polygonal somas adopting a microglial-like morphology as depicted by the dashed inserts (Figure 12C and E). Moreover, *in situ* hybridization was also performed on cryosectioned sagittal brain slices (Figure 13). In the cerebellum of PAFR WT a strong punctate labelling is observed. This signal is absent in the cerebellum of PAFR KO hippocampus. Further magnification of the PAFR WT cerebellum reveals that the punctate labelling appear to be present in the Purkinje and Granule cell layers of the cerebellar cortical lobule.

PAFR WT Sequencing Results

5’ - AAAGTTAGGGGGAAACTTAGCTCCACGCGTTGGGAGCTCTCCCATATGG

TCGACCTGCAGGCGGCCGCGAATTCACTAGTGATT**TATGGCTGACCTGCTCTT**

CCTGATCACCCTCCCACTGTGGTTGTCTACTACTACAACGAGGGCGACTGGA

TTCTACCCAACTTCCTGTGCAACGTGGCTGGCTGCCTCTTCTTCATCAATACC

TACTGCAGTGTGGCCTTTTTGGGTGTCATCACTTATAACCGCTACCAGGCAGT

AGCCTATCCCATCAAGACTGCACAGGCCACCACCCGCAAGCGTGGCATCTCT

TTGTCCCTGATCATTTGGGTATCCATTGTGGCTACTGCATCCTATTTCCTGGCC

ACAGACTCCACCAACCTAGTGCCCAATAAATCGAATTCCCGCGGCCGCCATG

GCGGCCGGGAGCATGCGACGTCGGGCCCAATTCG**CCCTATAGTGAGTCGTAT**

TACAATTCACTGGCCGTCGTTTTACAACGTCGTGACTGGGAAAACCCTGGCGT

TACCCAACTTAATCGCCTTGCAGCACATCCCCCTTTCGCCAGCTGGCGTAATAG

CGAAGAGGCCCGCACCGATCGCCCTTCCCAACAGTTGCGCAGCCTGAATGGC

GAATGGACGCGCCCTGTAGCGGCGCATTAAGCGCGGCGGGTGTGGTGGTTAC

GCGCAGCGTGACCGCTACACTTGCCAGCGCCCTAGCGCCCGCTCCTTTCGCT

TTCTTCCCTTCCTTTCTCGCCACGTTCGCCGGCTTTCCCCGTCAAGCTCTAAAT

CGGGGGCTCCCTTTAGGGTTCCGATTTAGTGCTTTACGGCACCTCGACCCCAA

AAAACTTGATTAGGGTGATGGTTCACGTAGTGGGCCATCGCCCTGATAGACGG

TTTTTCGCCCTTTGACGTTGGAGTCCACGTTCTTTAATAGTGGACT – 3’

Figure 11. PAFR WT 311 bp cDNA Sequencing. The 311 bp PAFR WT cDNA was ligated into a pGEM-T Easy Vector. Sequencing results (The Sprott Center for Stem Cell Research, University of Ottawa, Ottawa, ON) after cloning of pGEM-PAFR WT vector in JM109 Competent Cells. The sequence was compared usingnucleotide BLAST against mouse genomic + transcript. The red represents the sequence of 311 PAFR WT transcript used to generate the PAFR WT riboprobe. The highlighted cyan represents the T7 promoter sequence.

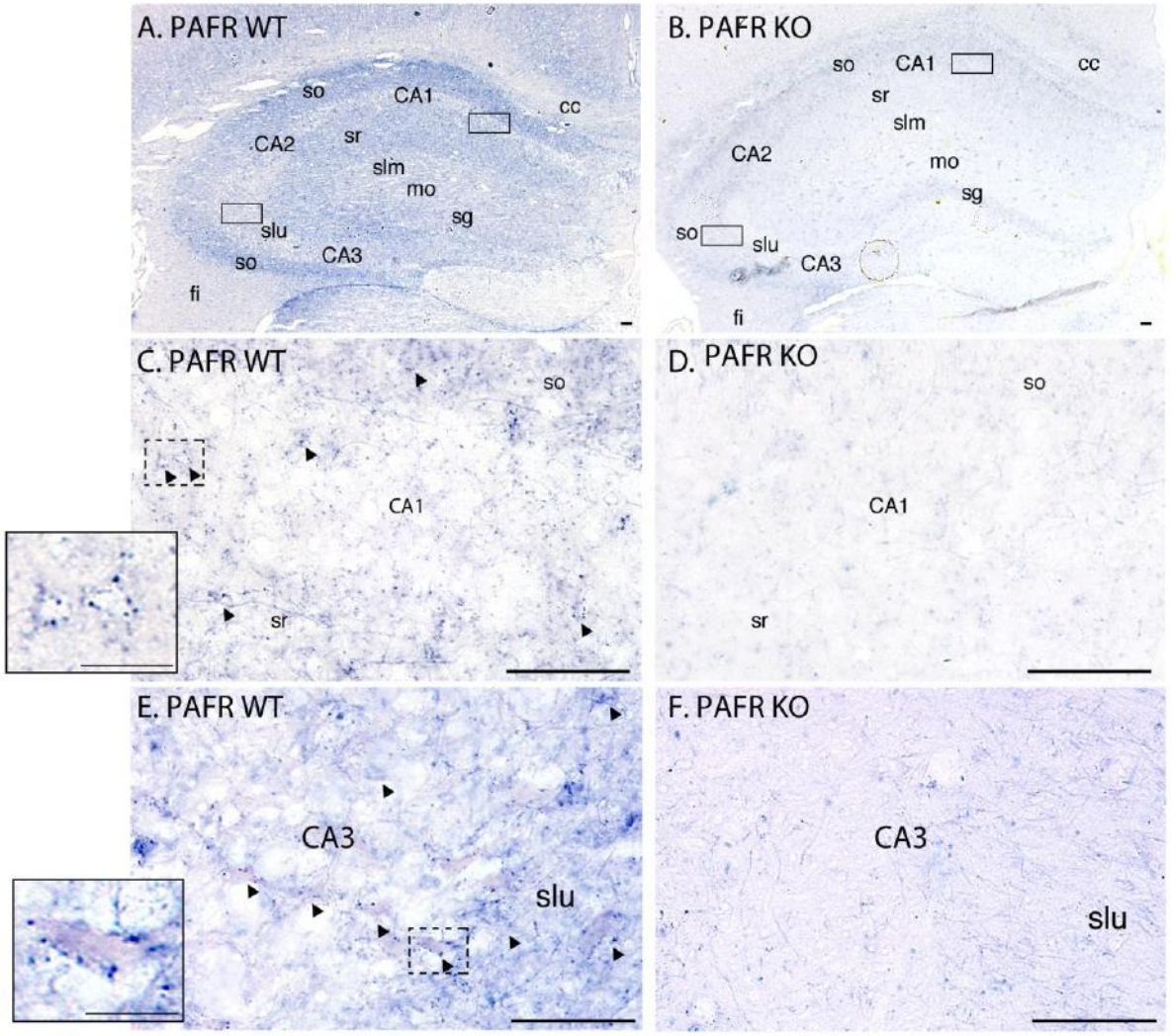

Figure 12.*In Situ* Hybridization of Coronal Section of Murine Hippocampus. PAFR WT riboprobe hybridized PAFR WT (left) and PAFR KO (right) mouse brain coronal sections depicting the hippocampus. Arrowheads represent microglial like morphology. Boxes in A indicate the positions of C and E. Boxes in B indicate the positions of D and F. Scale bar is 50 µm. The inserts in C and E represent higher magnification of dotted squares, where scale bar is 12.5 µm. Abbreviations: cc, corpus callosum; fi, fimbria; mo, stratum moleculare; sg, stratum granulosum; slm, stratum lacunosum; slu, stratum lucidem; so, stratum oriens; and sr, stratum radiatum.

Figure 13. *In Situ H*ybridization of Sagittal Section of Murine Brain.PAFR WT riboprobe hybridized PAFR WT and PAFR KO sagittal mouse brain section. A, represents entire sagittal brain section of PAFR WT. B and C depict hippocampus of PAFR WT (B) and PAFR KO (C) sagittal brain section of PAFR WT. D and E depict cerebellum of PAFR WT (D) and PAFR KO (E) sagittal brain sections. Scale bar for panels B-E is 50 μm.The scale bar for the inserts of panels D and E are 12.5 μm. Abbreviations: Acb, nucleus accumbens; Cb, cerebellum; cc, corpus callosum; CPu, striatum; Ctx, cerebral cortex; fi, fimbria; GL, Granular layer; HPF, hippocampal formation; ML, molecular layer; mo, stratum moleculare; PL, Purkinje layer; sg, stratum granulosum; slm, stratum lacunosum; slu, stratum lucidem; so, stratum oriens; sr, stratum radiatum; Thal, thalamus; VO, ventro orbital cortex.

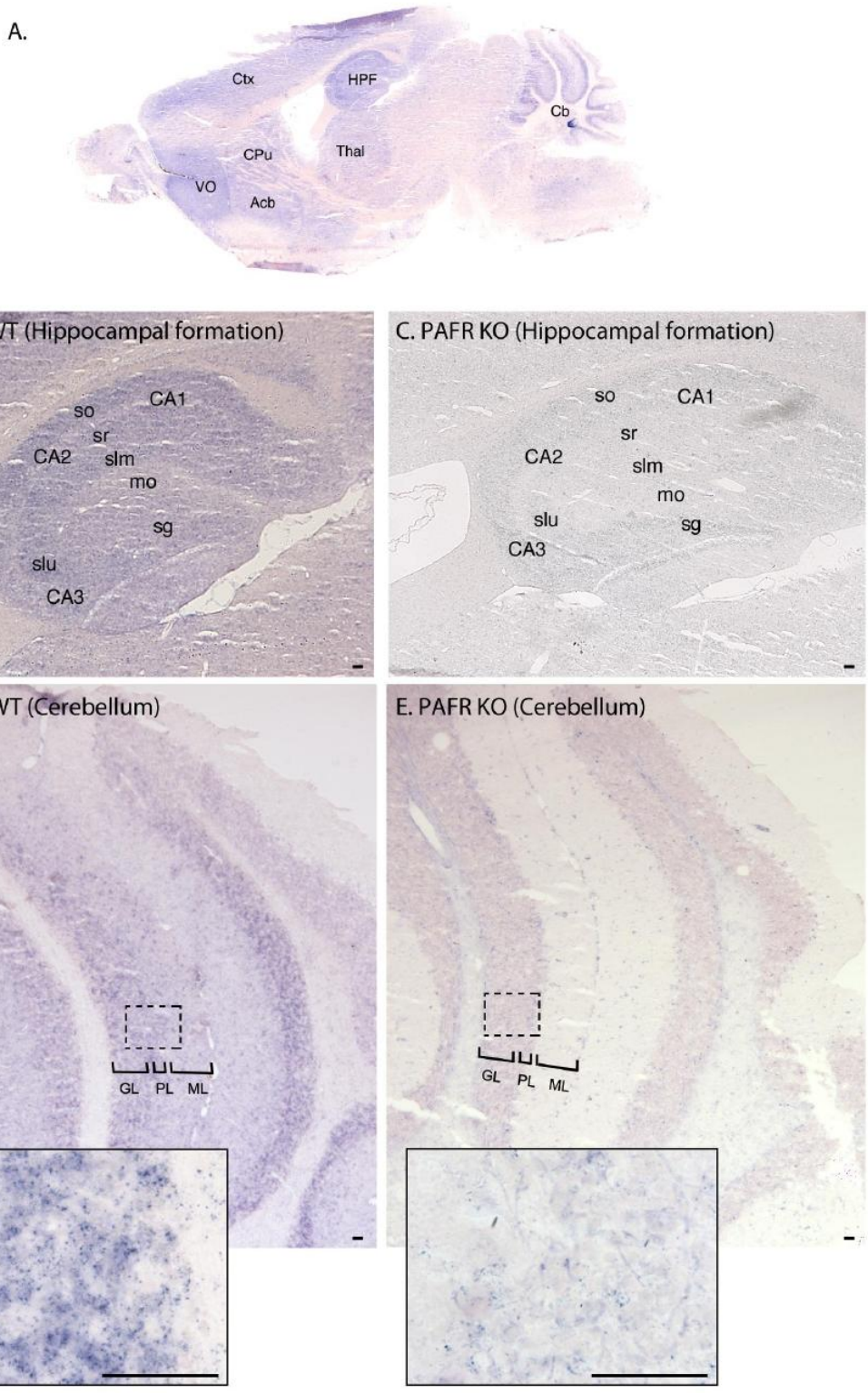
A.
Ctx
HPF
Cb
CPu
Thal
VO
Acb
B. PAFR WT (Hippocampal formation)
so
CA1
sr
CA2
slm
mo
sg
slu
CA3
C. PAFR KO (Hippocampal formation)
so
CA1
sr
CA2
slm
mo
slu
sg
CA3
D. PAFR WT (Cerebellum)
GL
PL
ML
E. PAFR KO (Cerebellum)
GL
PL
ML

Aim2 - Using a loss of function approach, to assess role of PAFR in hippocampal-dependent indices of learning and memory in mouse.

The objective of this aim was to evaluate the role of PAFR in learning and memory. The most widely used paradigm for evaluating learning and memory in rodents is the Morris water maze (MWM) analysis (Morris, 1984). Using this approach PAFR WT and KO mice were trained for eight consecutive days, where each day they were given four trials with randomized order of entrance. The learning and memory of mice was tested at the probe trial on the ninth day. The parameters that are analyzed in this investigation include average distance moved, average velocity of mice, average time spent in platform zone, average escape latency to find the platform, average escape latency upon Probe trial, and average thigmotaxis experienced by mice.

Distance Moved - The average distance moved was recorded for all eight training days. The value includes the average of the distances the mice swam within each of the four trials per day for eight days presented in centimetre (cm) values. It must be noted that the mice were given a duration of 60 seconds (sec) to swim for each trial. However if the mouse reached the platform before the 60 seconds were over, the time was automatically stopped along with the recording of swimming distance. In this experiment, six PAFR WT mice were tested and compared to five PAFR KO control mice. According to the results obtained, the average distance swam by the PAFR KO mice is significantly lower than that of PAFR WT mice (Figure 14A).

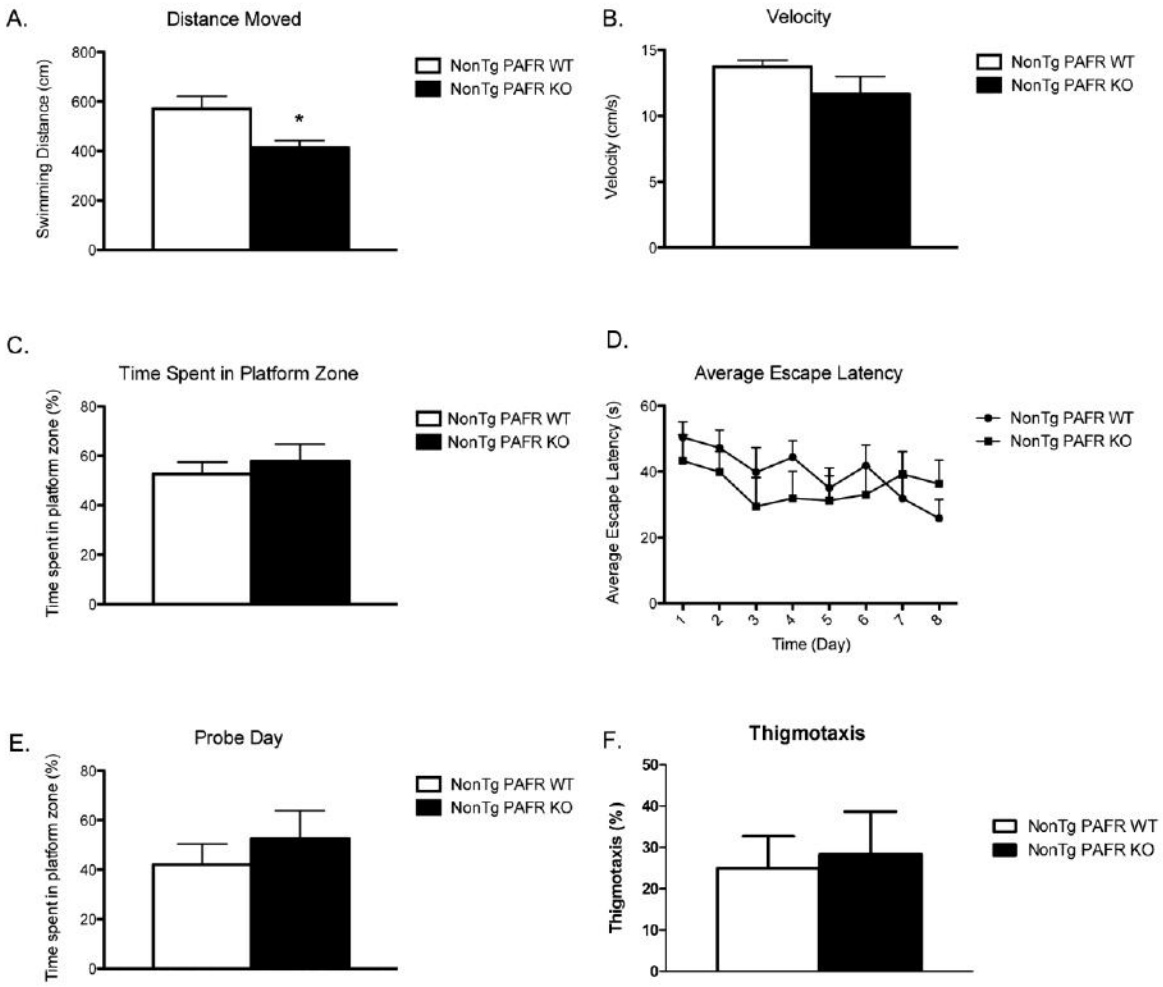

Figure 14. Morris Water Maze Analysis. Six NonTg PAFR WT and five NonTg PAFR KO mice were tested in the Morris water maze (MWM). Data depicting the average distance moved (A), the average velocity (B), the average time in Platform Zone (C), the average escape latency (D), Probe Trial (E), and thigmotaxis (F). The averages from A - D include the average of four trials per eight training days for all eight days +SEM. * p< 0.05 Student"s *t*-test (unpaired) was performed for all except D; ANOVA was performed for D.

Velocity - The averae swimming velocity of mice were recorded. Similar to the previous parameter, this measurement also includes the average velocity of all four trials for the duration of eight training days per mouse; where the values are presented as cm/s. As shown in Figure 14B, there is no statistical difference between the average velocities of PAFR WT mice compared to the PAFR KO mice.

Time in Platform Zone - The area within the pool where the platform was placed is referred to as the Platform Zone, which comprises of exactly one quarter of the entire pool. This parameter measures the average time the mice spent in the Platform Zone with respect to their total swimming time presented as percentage values. As with the previous distance and velocity measurements, these measurements also encompass the average time spent in the Platform Zone for each of the four trials for the entire eight training days. As evident by the results obtained, there appears to be no statistical difference observed in average time spent in Platform Zone between PAFR WT and KO mice (Figure 14C).

Escape Latency - This parameter measured the average escape latency of mice over the eight training days. Escape latency evaluated the learning curve of mice by assessing their ability to learn and remember the location of the hidden platform in the arena during these eight training days. These measurements include the daily averages of time the animals spent finding the hidden platform. As shown in Figure 14D, there appears to be no statistical difference between the average escape latency of PAFR WT mice compared to the PAFR KO. The escape latency of both PAFR WT and KO mice appears to decrease only moderately over time.

Probe Trial -The probe trial was conducted on the ninth day, immediately following the eight training days. At the probe trial, the hidden platform was removed, and mice were left to swim in the pool for the duration of 60 seconds. This measurement includes the time the mice spent in the Platform Zone with respect to the total sixty seconds of swimming time. As demonstrated in Figure 14E, there is no statistical difference evident in the average time spent in the Platform Zone between PAFR WT and KO mice.

Thigmotaxis - The final parameter to be examined in the MWM analysis was the average thigmotaxis experienced by mice. Thigmotaxis defines the percent of time the mice spent swimming in the pool‟s peripheral annulus, which is approximately within 25 cm from the pool walls. As per all other parameters that were investigated in this experiment, this measurement includes the average thigmotaxis experienced by mice within each four trials per day for the duration of eight training days presented as percentage values. The average thigmotaxis experienced by PAFR WT and KO are 24.97 ± 7.76 % and 28 ± 10.36 % respectively (Figure 14F). Furthermore, as evident by Figure 14F, there appears to be no statistical difference in thigmotaxis between the PAFR WT and KO mice.

Aim 3 - Using a loss of function approach, to determine whether loss of PAFR from microglia alters amyloid-beta plaque accumulation in a transgenic mouse model of AD.

The objective of this aim was to assess whether the impairment of PAFR elicits any effects on the number of amyloid-beta (Aβ) plaque accumulations characterizing AD in human. For this aim, a transgenic mouse model (TgCRND8) of AD was used along with PAFR KO mutant mice. TgCRND8 (Tg) mouse model of AD expresses a double mutant (KM670/671NL+V717F), Indiana and Swedish from the human APP under the control of the prion cos-tet promoter as previously described (Chishti et al., 2001). TgCRND8 mice were crossed with PAFR KO mice that are a hybrid C57BL/6J x 129/Ol background (Ishii et al., 1998). It should be noted that the PAFR KO mice were back-crossed for 4 generations into a C57BL/6 lineage in the Bennett laboratory before crossing with TgCNRD8 mice. The heterozygote offspring were bred with each other to generate the four congenic lines that were used for this study; TgPAFR KO, TgPAFR WT, NonTgPAFR KO, and NonTgPAFR KO.

Mice were sacrificed for analysis at 4 months, 6 months, and 8 months of age by lethal IPinjection with sodium pentobarbital. Upon sacrifice, brains were removed and cryosectioned (10 µm coronal sections). Immunofluorescence analysis was carried on the brain slices where Aβ plaques were quantified in four different regions of the brain (Anterior Cortex, Posterior Cortex, Basal Forebrain, and Hippocampus) using an antibody detecting both murine and human Aβ protein. The positions of the

photomicrographs taken (10X magnification) from each brain region that was studied are defined in Figure 9. Plaques were defined as immunoreactive compacted and spherical aggregates. The number of plaques in each field was documented and the total number of plaques summed across all fields to obtain a single measure per animal per region. The area of each region of interest was established and data was expressed as plaque counts/ mm^2 (Figure 15).

Anterior Cortex (AC) - The anterior cortex (AC) was one of the four regions of the murine brain to be assessed. Immunofluorescent detection of Aβ-reactive plaques in the AC of TgPAFR WT, TgPAFR KO, NonTgPAFR WT, and NonTgPAFR KO mice are depicted in Figure 15A and B. As evident in Figure 15A, there appears to be a positive trend between plaque number and age in both PAFR WT and KO mice. Conversely however, no statistical difference in plaque number is evident between PAFR WT and KO in any of the age groups. Furthermore, as depicted in Figure 15B, NonTg littermates exhibited very low Aβ-reactive plaques at all-time point of both PAFR WT and KO mice.

Posterior Cortex (PC) - The posterior cortex (PC) was the second region among the four to be assessed. As per AC analysis in the previous section, immunofluorescent detection of Aβ-reactive plaques in the PC of TgPAFR WT, TgPAFR KO, NonTgPAFR WT, and NonTgPAFR KO mice are demonstrated in Figure 15C and D. As shown in Figure 15C, similar to the observations detected in AC, there seems to be a positive trend between plaque number and age in both PAFR WT and KO mice. There appears to

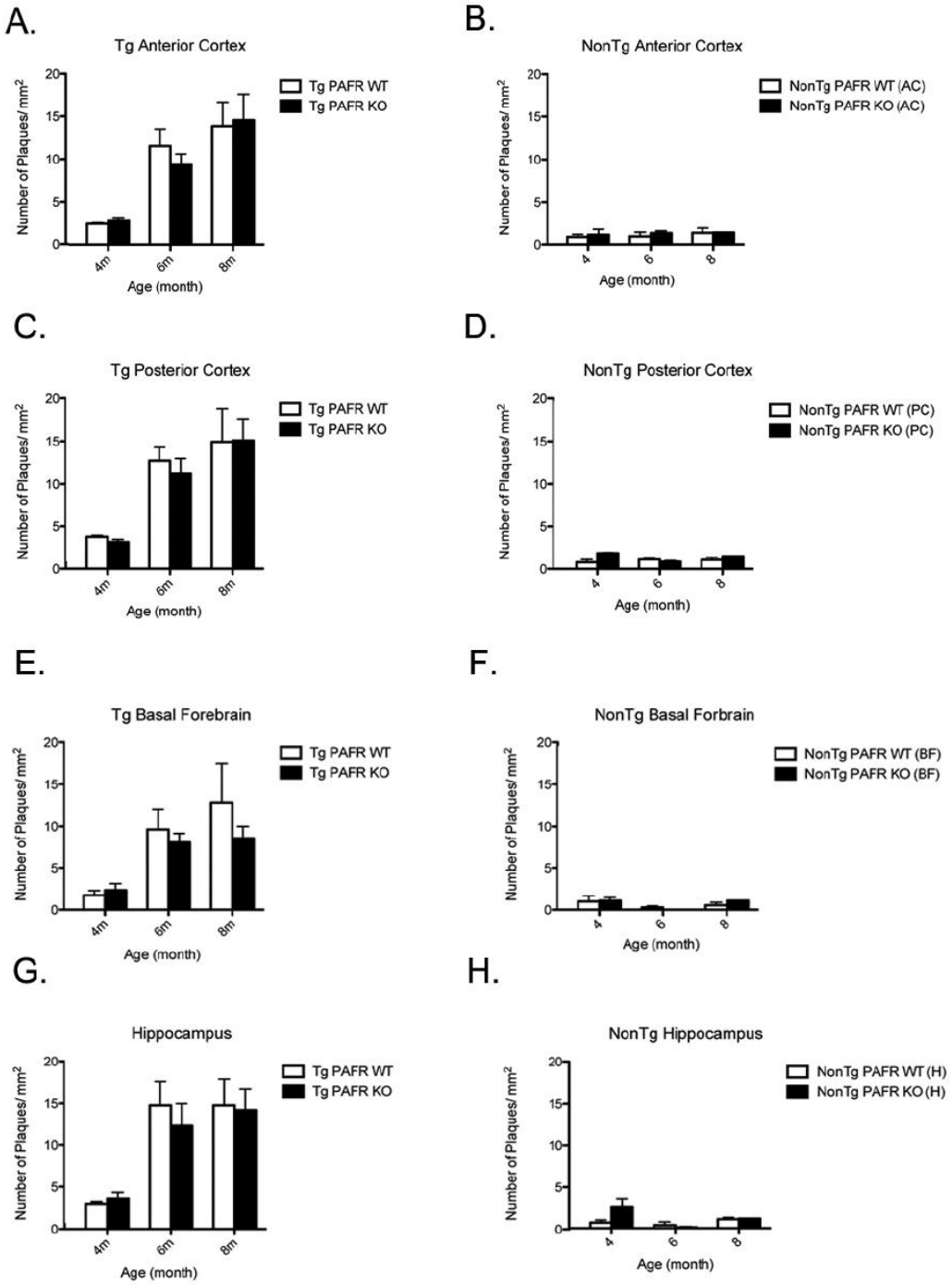

Figure 15. Time Dependant Aβ Plaque Accumulation. Aβ was detected in TgPAFR WT, TgPAFR KO , NonTgPAFR WT, and NonTgPAFR KO mice at 4, 6, and 8 months of age with the 4G8 antibody. Quantification of Aβ-reactive plaques at 2, 4, 6, and 8 months of age in TgPAFR WT, TgPAFR KO , NonTgPAFR WT, and NonTgPAFR KO mice in different brain regions ofTg and NonTg respectively: AC (A, B), PC (C, D),2BF (E, F) and H (G, H). Data represent mean number of plaques +SEM per 1 mm, ANOVA, *post-hoc* Tukey test was applied to detect statistical significance.

be no statistical difference in plaque number between PAFR WT and KO in any of the time points however. Moreover, as depicted in Figure 15D, minimal number of Aβ-reactive plaques are evident in the NonTg littermates at all age groups of both PAFR WT and KO mice.

Basal Forebrain (BF) - The third region that was examined in the anterior brain of murine was the basal forebrain (BF). Immunofluorescent detection of Aβ-reactive plaques in the BF of TgPAFR WT, TgPAFR KO, NonTgPAFR WT, and NonTgPAFR KO mice are depicted in Figure 15E and F. As illustrated in Figure 15E, a positive correlation between plaque number and age is observed in PAFR WT mice but not in PAFR KO mice. The number of plaques in PAFR KO appears to plateau from 4 to 6 months of age. Also, there is no statistical difference evident in plaque number between PAFR WT and KO at any of the time points. Moreover, as depicted in Figure 15F, NonTg littermates at all-time point exhibit very low number of Aβ-reactive plaques in both PAFR WT and KO mice.

Hippocampus (H) - The fourth region that was analyzed was the hippocampus at the posterior of the brain. Immunofluorescent detection of Aβ-reactive plaques in the hippocampus of TgPAFR WT, TgPAFR KO, NonTgPAFR WT, and NonTgPAFR KO mice are depicted in Figure 15G and H. A positive correlation between plaque number and age is evident in PAFR KO mice, whereas it is absent in the PAFR WT mice (Figure 15G). The number of plaques in PAFR WT seems to plateau from 4 to 6 months of age. Moreover, there is no statistical difference observed in plaque

number between PAFR WT and KO at any of the time points. Finally, as depicted in Figure 15H, NonTg littermates exhibit minimal number of Aβ-reactive plaques at all age groups in both PAFR WT and KO mice.

Chapter 4

DISCUSSION

In this thesis, I have shown that PAFR mRNA expression is likely localized to microglial-like cells in murine hippocampus. I also showed that PAFR mRNA is possibly localized to neuronal-like cells within the Purkinje and Granule cell layers of the murine cerebellum. I performed MWM analysis using wild-type mice and mice deficient in PAFR and observed that the loss of PAFR has no effect on learning and memory in mice; although this analysis was confounded by the observation that the MWM task parameters had not been optimized to detect a robust learning curve in WT mice. I further showed that the loss of PAFR in mouse model of AD has no effect on the number of Aβ plaque accumulation. The observations obtained in my thesis may provide preliminary insight to the reported differences in PAF-mediated effects on learning and memory in mice and rats.

Significant volumes of research targeting PAFR in the brain have emerged utilizing both rats and mice (Ishii and Shimizu, 2000). *In situ* hybridization experiments have shown that in rat brain, PAFR mRNA is localized to a subset of neurons however predominantly to microglia (Mori et al.,1996, Bennett et al., 1998). Similar studies using Northern blot analysis support that PAFR mRNA is present in mouse brain as well (Ishii et al., 1996). However unlike rats, no further characterizations have been conducted to determine where in mouse brain PAFR mRNA is localized.

This is rather intriguing since there are contradictory observations reported from electrophysiology experiments performed on rats and mice brains targeting PAFR. The rat study by Kato *et al.* reported that PAFR plays a role in LTP induction in rat hippocampus, and they hypothesized that PAF may be a retrograde messenger traveling from the post-synaptic neuron to the pre-synaptic neuron (Kato et al., 1994). Conversely, Kobayashi *et al.* performed electrophysiology experiment in mice lacking PAFR and presented contradicting results (Kobayashi et al., 1999). The findings of Kobayashi *et al*. regarding electrophysiology experiments suggested that PAFR is not required for LTP induction in mouse hippocampus. The suggestion that PAFR plays no role in LTP induction in mice was later contradicted by another study performed by Chen *et al*. who reported that LTP is attenuated in mice deficient in PAFR (Chen et al., 2001). The findings of Chen *et al*. raise questions in regards to the role of PAFR in LTP induction and subsequently learning and memory in mice. This begs the question - whether the contradictory data observed in rats and mice are simply due to PAFR expression being rodent specific.

In pursuit to providing an explanation to this question, I performed *in situ* hybridization to localize PAFR mRNA in mouse hippocampus. *In situ* hybridization was performed on murine coronal brain slices of PAFR WT and PAFR KO controls. The signals in the PAFR WT CA1 and CA3 of the hippocampus appeared to exhibit small polygonal somas adopting a microglial-like morphology. Since these signals were absent in the PAFR KO control tissues, it is perhaps plausible to state that these signals are specific to some brain structures. To support this observation, follow-up validation experiments must be pursued including combining *in*

*situ*hybridization with immunohistochemistry targeting antigens specific for microglia. In the case of microglia, cell specific markers that can be used include Iba 1 (ionized calcium binding adaptor molecule 1) and Ox-42 (type 3 complement receptor) (Sasaki et al., 2001; Ling et al., 1990). The latter is most often used for the detection of activated microglia, a surface receptor that is especially upregulated upon microglia morphology change from ramified to amoeboid (Ling et al., 1990). The former is an actin cross linking protein specific to microglia and is upregulated upon microglial activation; which is generally used for the detection of ramified as well as amoeboid microglia (Sasaki et al., 2001).

In situ hybridization was also performed on cryosectioned sagittal brain slices. In the cerebellum of PAFR WT tissue, a strong punctate labelling is observed in the Purkinje and Granule cell layers of the cerebellar cortical lobule. The signals adopt a neuronal-like morphology which is absent in the cerebellum of PAFR KO hippocampus. Since ramified microglia reside in all three layers of the cerebellar lobules and the distribution in these layers is scattered rather than homogenous, one may speculate that it is more likely that these signals are from neurons than from microglia (Vela et al., 1995). However, it must be noted that within the Purkinje and Granule cell layers four different types of neurons are documented including, Purkinje, Granule, Golgi, and Basket cells (Ramnani, 2006). As the PAFR KO control cerebellum was void of this signal, it is perhaps reasonable to state that these signals are specific to some brain structures. Follow-up validation experiments must be pursued to confirm that these punctate signals are from neurons, including combining *in situ* hybridization with immunohistochemistry to detect antigens specific

to neurons. A frequently used antigen for the detection of neurons is NeuN, which is a neuronal nuclear marker (Mullen et al., 1992). Additional classification of neuron type can be made based on morphology analysis - as each type of neuron has a distinct morphology. Finally, specific conclusions can be drawn upon using antigens that are neuron-type specific; such as the case of Zerbin II, a marker for Adolase C, specifically expressed in Purkinje cells (Ginzburg and Futerman, 2005).

The goal of the first aim was to localize PAFR mRNA in murine hippocampus. A molecular approach was pursued to achieve this goal; as a particular transcript of PAFR was utilized to generate a specific riboprobe and yielded no signal in PAFR KO controls. It is worthy of mention however, that an immunological approach can also be taken to further confirm the data and fluorescence activated cell sorting (FACS) presents a rather useful tool in pursuing such goal. The tissue of interest, in this case hippocampus, may be dissected and subpopulations of cells can be sorted and separated based on markers of interest, in this case antigens for microglia and neurons. Once cells have been sorted, RNA and protein may be detected to document PAFR expression. Confirmation and validation of PAFR mRNA and protein localization in murine hippocampus is important for determining the role of PAFR in learning and memory in mice.

As per the observations that I obtained from this thesis, the suggestion that PAFR mRNA is possibly localized to microglial-like cells in mouse hippocampus supports the findings of Kobayashi *et al*."s electrophysiology experiments. If PAFR were strictly localized to microglia and not neurons in mouse hippocampus, then it is

plausible to conclude that PAFR may have no role in LTP induction in mouse hippocampus. The observations obtained from the MWM experiment in the second aim provide some support, albeit preliminary for this suggestion. In the MWM experiment, the mice lacking PAFR did not exhibit any statistical differences in learning and memory compared to their wild-type littermates, although both lines did not show a robust learning curve.

In the MWM experiment, six parameters were analyzed including: the average distance moved, the average velocity of mice, the average time spent in platform zone, the average escape latency to find the platform, the average escape latency upon probe trial, and the average thigmotaxis experienced by mice. The average distance swam by the PAFR KO mice was significantly lower than that of PAFR WT mice. This indicates that on average, mice lacking PAFR did not swim as far as their PAFR WT littermates. This suggests a few possibilities. One may argue that perhaps these PAFR KO mice were far too anxious to swim leading them to remain floating and stationary. This interpretation is however unlikely, as percent thigmotaxis did not differ between PAFR WT and KO mice. Thigmotaxis defines the percent of time the mice spent swimming in the pool‟s peripheral annulus, which is approximately within 25 centimeters from the pool walls. Thigmotaxis has been used as an index of anxiety or fear in rodents (Barnett, 1968; Simon et al., 1994). In fact, it has been suggested that the anxiety experienced by the animals allegedly interferes with their performance and ability to engage in a productive navigational schemes in the MWM *(Devan et al., 1999).* However, the average thigmotaxis experienced by PAFR KO mice was not different than wild-type. Taken together, these data suggest that

thigmotaxis cannot explain the difference in distance between PAFR KO and WT mice and further experiments are necessary. Moreover, it is also possible that PAFR KO mice are physiologically limited compared to the PAFR WT mice. From previous published studies however, the phenotype of PAFR KO mice appears to be normal (Ishii and Shimuzu, 2000).

Another parameter that was analyzed in the MWM paradigm was velocity. There was no statistical difference observed between the average velocities of PAFR WT mice compared to the PAFR KO mice. This indicates that statistically both the PAFR KO and PAFR WT mice swam about the same velocity, though on average, PAFR KO had swam significantly less distance. It should be reminded that in each training session, the mice were given 60 seconds of swimming time counting up, and the instance the mice stepped on the platform and remained there for two seconds the timer was stopped. Therefore, a possibility may be that the PAFR KO mice simply found the target in a shorter time than the PAFR WT, and so did not need to swim much further in attempts of finding the hidden platform. This could provide an explanation to why PAFR KO mice moved less distance but had almost equal velocity to their PAFR WT littermates.

Escape latency analysis was another parameter that was assessed as it evaluated the performance of mice in locating the hidden platform in the duration of eight training days. The escape latency of PAFR KO mice seemed to decrease over the first three days, and began to increase for the rest of the remaining five days, reaching the initial level (escape latency at day one) by the eighth day. The initial

level of escape latency of PAFR WT mice was surprisingly slightly higher than that of PAFR KO. Unlike PAFR KO however, the escape latency of PAFR WT mice appeared to decrease over the eight training days. This is in agreement with the idea that overall it took less time for PAFR KO mice to find the hidden platform, however unlike their PAFR WT littermates, they did not improve on learning and remembering where the hidden platform was overtime. It is essential to note however, that the overall learning curves were not statistically different and that initial escape latencies at Day 1 were already extremely low suggesting that the best parameters had not been optimized to detect learning and memory robustly. The task was simply too easy for this strain of mouse and further studies must consider reducing the number of cues available to the animals to increase difficulty. Suggested alternations are described below. These results imply that perhaps PAFR in mice is not required for special learning and memory. Although conclusions cannot be drawn since the PAFR WT controls did not elicit a reliable learning curve. Studies indicate that an ideal learning curve should exhibit a drop by at least a half if not more by the last day of training (Zhou et al. 2009; Wolfer et al., 1998).

The most important limitation of the MWM experiment is the observation that the PAFR WT did not in fact produce a dependable positive control. The escape latency of PAFR WT mice appeared to decrease over time however not by at least a half, as studies demonstrate (Zhou et al. 2009; Wolfer et al., 1998). In this MWM experiment, the PAFR WT mice spent approximately 48 sec to escape from water on the first day of training, and they managed to spend only 1.4 times (33 sec) less by the last day of training. This observation further indicates that the PAFR WT mice

were already too competent at day one, taking them on average only 48 sec to reach the platform, whereas other studies report average escape latency of much higher time at day one (Wolfer et al., 1998).

A few factors that may influence the performance of mice in MWM include the number of trials per day, duration of each trial and inter-trial intervals, the number of days of training, and the preparations of mice prior to training (Sharma et al., 2010; Zhou et al. 2009).In this MWM investigation 4 trials were performed for each day of training, perhaps 3 or 2 trials per day would have elicited more ideal outcomes. In addition, in this MWM analysis two visual cues were present the entire duration of the experiment; perhaps the test would be more challenging if the extra cues were removed. Too many random "unwanted" and inconsistent cues around and above the pool may have skewed the results as well. The room where MWM is performed at should be void of any extra and inconsistent clues for the duration of the experiment.

Previous studies indicate that in the MWM paradigm, two-third of behavioural variability among individual mice is due to non-cognitive factors such as reduced swimming speed and thigmotaxis (Wolfer et al., 1998). The latter has been accounted for. The thigmotaxis values of both PAFR WT and KO are below 30% which is considered reasonable. This supports the suggestion that thigmotaxis did not play a significant role in these results. Therefore perhaps the reduction in swimming speed and the subsequent floating observed in mice were due to hypothermia emerging in mice during the MWM test. Indeed, body temperature of

mice swimming in a MWM experiment may drop by 9°C, which is correlated to decline in swimming speed (Iivonen et al., 2003). Studies suggested that mice must be given at least 13 minutes of inter-trial intervals and raise the water temperature to 24-26°C in order to limit hypothermia (Iivonen et al., 2003; Morris et al., 1984). It must be noted however, that in our experiment the temperature of water was 21 ± 1°C at all times and mice were given 20 minutes of inter-trial intervals between each trial. Although 20 minutes of inter-trial intervals may have been sufficient to bring the body temperature of mice back to normal, perhaps the water temperature should have been slightly higher. In addition, variability may still lie in that some mice had greater body fat than others and as a result were better equipped for possible hypothermia (Iivonen et al., 2003). The body weight or body temperatures of mice however were not documented; therefore it cannot be concluded for certain whether hypothermia played a role in the results obtained. Finally, an obvious factor that may assume as a limitation to these results is the sample size used in the experiment. Six mice for PAFR WT and five for PAFR KO are limited sizes.

Aim one in my thesis sought to localize PAFR mRNA in mouse brain, and concluded that PAFR mRNA is indeed evident in mouse brain and most likely in cells with microglial-like morphology. As mentioned earlier, amoeboid or rather activated microglia have an important role in AD as they have chemotaxic abilities and secrete various proteases that degrade Aβ plaques. As such, PAF-mediated chemotaxis of microglia has been shown to be impaired in PAFR KO mice (Aihara et al., 2000). Therefore the goal of the third aim was to assess whether this impairment impacts

upon the accumulation of Aβ plaques in a transgenic model of AD.

In all four regions of the brain that I studied, there appeared to be no statistically significant difference in the number of plaques detected between PAFR WT and PAFR KO mice in all three time points. However there was an overall positive trend between the number of plaques and time as expected and consistent with the literature since AD is an age dependent disease and plaques accumulate over time (Selkoe, 2001). Aβ plaque accumulation over time occurs as a result of an imbalance between Aβ production and clearance. In humans, accumulation of Aβ deposits takes place in a hierarchical fashion with respect to distinct areas of the brain, for example two regions that are affected earliest in the course of AD are the perirhinal/entorhinal cortex and the hippocampus (Thal et al., 2000). In my findings however, I observe a global accumulation of Aβ plaque deposits at a fairly consistent rate throughout the brain- at least among the regions of the brain that were analyzed in this study. This is not entirely unexpected however. Due to the constitutive promoter in the mouse model, APP processing is impaired to equal extent in all neurons and glia throughout the brain whereas in the human disease, Aβ deposition, for example, in the posterior cortex precedes hippocampal involvement (Chishti et al., 2001; Thal et al., 2000). As per the results obtained, a role for PAFR in plaque processing was not apparent in any of the time points suggesting that the absence of the receptor has little effect on Aβ plaque number. It further indicates that the loss of PAFR within microglial-like cells has no effect on Aβ degradation; PAF being one of the activators of microglia (Johnson et al., 2004).

In this study, the Aβ plaque counts were conducted by selecting all compacted and spherical aggregates visible after immunofluorescence staining with the antibody 4G8-which detects residues 17 to 24 of Aβ peptide. As mentioned previously, aberrant processing of mutated APP leads to the production of an excess of the 42 amino acid form of Aβ($A\beta_{42}$). This $A\beta_{42}$ undergoes a cascade of structural changes to finally elicit the aggregated Aβ plaque. Initially alpha-helical in conformation, $A\beta_{42}$ adopts a β-sheet secondary structure due to the large number of hydrophobic amino acids. In presence metal ions, the β-sheet secondary structures of $A\beta_{42}$ oligomerize and form toxic oligomers (Jarrett et al., 1993; Walsh et al., 2000). These oligomers, in turn, aggregate to form proto-fibrils, which are also very toxic and themselves aggregate together to form fibrils. Numerous fibrils stick together and generate Aβ plaques (Walsh et al., 1999). The antibody used detected any one of these assemblies of Aβ; which indicates that my Aβ counts are not limited to plaques. Although it was possible to measure diameters of these spherical aggregates, exact identification of the Aβ-reactive aggregates were not made.

The third aim sought to determine whether the loss of PAFR from microglia affects Aβ plaque number in a mouse model (Tg) of AD. It should be noted that activated microglia are the major source of inflammatory mediating factors in neurodegenerative diseases like AD (Farfara et al., 2008). Microglial activation is regulated by stimulation of microglia with cytokines (IL-1β, IL-6, TNFα, and etc.) chemokines, and lipid autacoids such as PAF (Nakamura, 2002). In AD, once microglial cells are activated they aggregate around Aβ-plaques (Gehrmann et al., 1995). Frequent accumulation of microglia around mature senile plaques is invariably detected in post-mortem AD

tissue; however, this accumulation may indicate an attempt with limited access of Aβ removal. It is supposed that continued activation of microglia in these lesions would elicit a persistent inflammatory response (Akiyama, 1994). One mean by which microglia impact amyloid plaque number and size is through the release of Aβ degrading enzymes such as neprilysin, activated by microglia (Simard and Rivest, 2006; Tanzi, 2004). Acute microglial accumulation is associated with the clearance of Aβ oligomers and plaques through synthesis and release of the Aβ degrading enzyme neprilysin (Hickman et al., 2008). Chronic accumulation, however, is associated with a decrease in neprilysin expression (Hickman et al., 2008). In our studies, loss of PAFR did not have any significant effect on the rate of Aβ plaque number. The measure of the rate of microglial activation would support this notion. The activation of microglial PAFR by PAF elicits a powerful chemotactic response (Pettorossi et al., 2001). Although impairment of the chemotactic response of microglia has been reported in PAFR KO mice, no direct evidence has been presented to suggest that the loss of PAFR impairs activation of microglia (Aihara et al., 2000). Quantification of the number of Aβ provides limited support for the involvement of microglial activation in plaque removal and/or formation. Compensatory mechanisms leading to microglia activation in the absence of PAFR is a possibility. As such, quantification of activated microglia as well as neprilysin could be examined in future studies.

CONCLUSIONS

Reported studies suggest that PAFR may be responsible for LTP induction in rat hippocampus; and that in rat, PAFR may be implicated in learning and memory (Wieraszko et al., 1993; Kato et al., 1994; Izquierdo et al., 1995). In fact, a study by Kato *et al*. provides evidence that PAF may be a candidate for a retrograde messenger-crossing the synaptic cleft from the post synaptic neuron to the presynaptic neuron (Kato et al., 1994). If PAF were a retrograde messenger as Kato *et al*. suggest, then this implicitly indicates that PAFR must be localized to neurons, at least at the presynaptic cleft. In rat, this is a plausible suggestion since it has been shown that PAFR mRNA expression is localized to subset of neurons in the CA1 region of the hippocampus (Mori et al., 1996, Bennett et al., 1998). As described earlier, the findings of Kobayashi *et al*. derived from electrophysiology experiments demonstrated that PAFR is not required for LTP induction in mouse hippocampus (Kobayashi et al., 1999). This idea was later contradicted as another study by Chen *et al*. reported that LTP is attenuated in PAFR KO mice (Chen et al., 2001). These reported differences in the role of PAFR in LTP induction suggested that perhaps PAFR expression is rodent-specific. Therefore my thesis hypothesized that PAFR expression is restricted to microglia in mouse hippocampus and that this restriction would underlie these reported differences derived from electrophysiology experiments conducted in rats and mice.

My thesis has showed that PAFR mRNA expression is localized to cells with microglial-like morphologies in the mouse hippocampus, although further analysis is

needed to verify that the observed signal is from microglia. Although I did not perform any electrophysiology experiments, the suggestion that PAFR is possibly localized to microglial like cells leads me to conclude that perhaps PAFR has no role in LTP induction in mice as Kobayashi *et al*. suggested. This conclusion can be further supported by the findings of the MWM analysis that I performed using PAFR WT and KO mice; loss of PAFR in mice had no significant impact upon learning and memory.

Furthermore, as described previously, activated microglia have an important role in AD as they have chemotaxic abilities and secrete various proteases that degrade Aβ plaques (Gehrmann et al., 1995). PAF-mediated chemotaxis of microglia has been shown to be impaired in PAFR KO mice (Aihara et al., 2000). Therefore the last objective of my thesis was to determine whether the loss of PAFR impacts upon the accumulation of Aβ plaques in a transgenic model of AD. My findings demonstrated that PAFR has no significant role in the number of Aβ plaque accumulation. Collectively my observations suggest that PAFR expression is restricted to microglial-like cells in mouse hippocampus and that loss of PAFR has no effect on learning and memory or Aβ plaque number in mouse model of AD. My observations provide partial support for Kobayashi *et al.*'s study, suggesting that PAFR has no role in LTP induction and subsequently learning and memory in mice, although these conclusions remain confounded by the failure of the MWM task to measure learning and memory robustly under the conditions described in this thesis.

REFERENCES

Aihara, M., Ishii, S., Kume, K., and Shimizu, T. (2000) Interaction between neurone and microglia mediated by platelet-activating factor. Geness.Cell.*5*, 397-406.

Akiyama H. (1994) Inflammatory response in Alzheimer's disease. Tohoku. J. Exp. Med.*174*, 295-303.

Alonso, F., Gil, M.G., Sánchez-Crespo, M., and Mato, J.M.(1982) Activation of 1-alkyl-2-lyso-glycero-3-phosphocholine-acetyl-CoA transferase during phagocytosis in human polymorphonuclear leukocytes.J. Biol. Chem. *257*, 3376-3378.

Bazan, N.G., Packard, M.G., Teather, L., and Allan, G. (1997) Bioactive lipids in excitatory neurotransmission and neuronal plasticity. Neurochem. Int.*30*, 225-231.
Barnett SA. (1963) The Rat: A Study in Behaviour. Chicago: Aldine, pp.288.

Bennett, S.A., Chen, J., Pappas, B.A., Roberts, D.C., and Tenniswood, M. (1998) Platelet activating factor receptor expression is associated with neuronal apoptosis in an *in vivo* model of excitotoxicity. Cell.Death. Differ. *5*, 867-875.

Benveniste, J., Henson, P.M., and Cochrane, C.H. (1972) Leukocyte-dependent histamine release from rabbits platelets.The role of IgE, basophils, and a platelet activating factor. J. Exp. Med.*136*, 1356-1377.

Bertram, L., Lill, C.M., and Tanzi, R.E. (2010) The genetics of Alzheimer disease: back to the future. Neuron.*68*, 270-281.

Bito, H., Honda, Z., Nakamura, M. and Shimizu, T. (1994) Cloning, expression and tissue distribution of rat platelet-activating-factor-receptor cDNA. Eur. J. Biochem. *221*, 211-218.

Bito, H., Nakamura, M., Honda, Z., Izumi, T., Iwatsubo, T., Seyama, Y., Ogura, A., Kudo, Y., and Shimizu, T. (1992) Platelet-activating factor (PAF) receptor in rat brain: PAF mobilizes intracellular Ca2+ in hippocampal neurons. Neuron.*9*, 285-294.

Blank, M.L., Cress, E.A., Lee, T.C., Malone, B., Surles, J.R., Piantadosi, C., Hajdu, J., and Snyder, F. (1982). Structural features of platelet activating factor (1-alkyl-2-acetyl-sn-glycero-3-phosphocholine) required for hypotensive and platelet serotonin responses. Res. Commun. Chem. Pathol. Pharmacol.*38*, 3-20.

Blank, M.L., Snyder F., Byers L.W., Brooks B., and Muirhead E.E. (1979) Anti-hypertensive activity of an alkyl ether analog of phosphatidylcholine.Biochem.Biophys. Res. Commun. *90*, 1194-1200.

Bliss, T.V., and Collingridge, G.L. (1993) A synaptic model of memory: long-term potentiation in the hippocampus. Nature. 361, 31-39.

Borst, P., Zelcer, N., and van Helvoort, A. (2000). ABC transporters in lipid transport. Biochim.Biophys.Acta.*1486*, 128-144.

Bratton, D. and Henson, P.M. (1989) In: P.J. Barnes, C.P. Page and P.M. Henson, Editors, Platelet Activating Factor and Human Disease, In: P.J. Barnes, C.P. Page and P.M. Henson, Editors, Blackwell Scientific Publications, London, pp. 23-57.

Brown, S.L., Jala, V.R., Raghuwanshi, S.K., Nasser, M.W., Haribabu, B., and Richardson, R.M. (2006) Activation and regulation of platelet-activating factor receptor: role of G(i) and G(q) in receptor-mediated chemotactic, cytotoxic, and cross-regulatory signals. J. Immunol.*177*, 3242-3249.

Bussolino, F., Gremo, F., Tetta, C., Pescarmona, G.P., and Camussi, G.(1986) Production of platelet activating factor by chick retina. J. Biol. Chem. *261*, 16502-16508.

Camussi, G., Tetta, C., and Baglioni, C. (1990) The role of plateletactivating factor in inflammation. Clin.Immunol.Immunopathol.*57*, 331-338.

Carolan, E.J., and Casale, T.B. (1990) Degree of platelet activating factor-induced neutrophil migration is dependent upon the molecular species. J. Immunol. *145*, 2561-2565.

Chao, W., and Olson, M.S. (1993) Platelet-activating factor: receptors and signal transduction.Biochem.*292*, 617-629.

Chen, C., Magee, J.C., Marcheselli, V., Hardy, M., Bazan, N.G. (2001) Attenuated LTP in hippocampal dentate gyrus neurons of mice deficient in the PAF receptor. J. Neurophysiol. *85*, 384-390.

Chishti, M.A., Yang, D.S., Janus, C., Phinney, A.L., Horne, P., Pearson, J., Strome, R., Zuker, N., Loukides, J., French, J., Turner, S., Lozza, G., Grilli, M., Kunicki, S., Morissette, C., Paquette, J., Gervais, F., Bergeron, C., Fraser, P.E., Carlson, G.A., George-Hyslop, P.S., and Westaway, D. (2001) Early-onset amyloid deposition and cognitive deficits in transgenic mice expressing a double mutant form of amyloid precursor protein 695. J. Biol. Chem. *276*, 21562-21570.

Citron, M. (2004) Strategies for disease modification in Alzhiemer's disease. Nature. Reviews.*5*, 677-685.

Clark, G.D., Happel, L.T., Zorumski, C.F., and Bazan, N.G. (1992) Enhancement of hippocampal excitatory synaptic transmission by platelet-activating factor. Neuron.*9*, 1211-1216.

Dagenais, P., Thivierge, M., Parent, J.L., Stankova, J., and Rola-Pleszczynski, M. (1997) Augmented expression of platelet-activating factor receptor gene by TNF alpha through transcriptional activation in human monocytes. J. Leukoc. Biol. *61*, 106-112.

Devan, B.D., McDonald, R.J., and White, N.M. (1999) E!ects of medial and lateral caudate-putamen lesions on place- and cue guided behaviors in the water maze: relationto thigmotaxis. Behav.Brain. Res. *100*, 5-14.

De Strooper, B. and Annaert, W. (2000) Proteolytic processing and cell biological functions of the amyloid precursor protein. J. Cell. Sci. *113*, 1857-1870.

Dyer, K.D., Percopo, C.M., Xie, Z., Yang, Z., Kim, J.D., Davoine, F., Lacy, P., Druey, K.M., Moqbel, R., and Rosenberg, H.F. (2010) Mouse and Human Eosinophils Degranulate in Response to Platelet-Activating Factor (PAF) and LysoPAF via a PAF-Receptor-Independent Mechanism: Evidence for a Novel Receptor. J. Immunol. *184*, 6327-6334.

Erger, R.A., and Casale, T.B.(1996) Eosinophil migration in response to three molecular species of platelet activating factor.Inflamm. Res. *45*, 265-267.

Ernest, S., and Bello-Reuss, E. (1999) Secretion of platelet-activating factor is mediated by MDR1 P-glycoprotein in cultured human mesangial cells. J. Am. Soc. Nephrol.*10*, 2306-2313.

Farfara, D., Lifshitz, V., and Frenkel, D.(2008) Neuroprotective and neurotoxic properties of glial cells in the pathogenesis of Alzheimer's disease.J. Cell. Mol. Med.12, 762-780.

Finder, V.H. and Glockshuber, R. (2007) Amyloid-beta aggregation.Neurodegener. Dis. *4*, 13-27.

Florent-Béchard, S., Desbène, C., Garcia, P., Allouche, A., Youssef, I., Escanyé, M.C., Koziel, V., Hanse, M., Malaplate-Armand, C., Stenger, C., Kriem, B., Yen-Potin, F.T., Olivier, J.L., Pillot, T., and Oster, T. (2009) The essential role of lipids in Alzheimer's disease. Biochimie.*91*, 804-809.

Franklin, R.A., Mazer, B., Sawami, H., Mills, G.B., Terada, N., Lucas, J.J., and Gelfand, E.W. (1993) Platelet-activating factor triggers the phosphorylation and activation of MAP-2 kinase and S6 peptide kinase activity in human B cell lines. J. Immunol.*151*, 1802-1810.

Farooqui A. A., Farooqui, T., and, Horrocks, L. A. (2008) Chapter 9:Roles of Platelet - Activating Factor in Brain. In: Metabolism and functions of bioactive ether lipids in the brain. Springer Science and Business Media, LLC. USA. pp. 171- 195.

García Rdríguez, C., Cundell, D.R., Tuomanen, E.I., Kolakowski, L.F. Jr., Gerard, C., and Gerard, N.P. (1995) The role of N-glycosylation for functional expression of the human platelet-activating factor receptor. Glycosylation is required for efficient membrane trafficking. J. Biol. Chem. *270*, 25178-25184.

Gatz, M., Reynolds, C.A., Fratiglioni, L., Johansson, B., Mortimer, J.A., Berg, S., Fiske, A., and Pedersen, N.L. (2006).Role of genes and environments for explaining Alzheimer disease. Arch. Gen. Psychiatry. *63*, 168-174.

Gehrmann, J., Matsumoto, Y., and Kreutzberg, G.W. (1995) Microglia: intrinsic immuneffector cell of the brain. Brain. Res. Brain. Res. Rev. *20*, 269-287.

Ginzburg, L., and Futerman, A.H. (2005) Defective calcium homeostasis in the cerebellum in a mouse model of Niemann-Pick A disease. J. Neurochem.*95*, 1619-1628.

Grösgen, S., Grimm, M.O., Friess, P., and Hartmann, T. (2010) Role of amyloid beta in lipid homeostasis.Biochim.Biophys.Acta.*180*, 966-974.

Handa, R.K., Strandhoy, J.W., and Buckalew, V.M. Jr.(1991) Vasorelaxant effect of C16-PAF and C18-PAF on renal blood flow and systemic blood pressure in the anesthetized rat.Life. Sci. *49*, 747-752.

Herbert, J.M. (1992). Characterization of specific binding sites of 3H-labelled platelet- activating factor ([3H]PAF) and a new antagonist, [3H]SR 27417, on guinea-pig tracheal epithelial cells. Biochem. J. *284*, 201-206.

Herrup, K. (2010) Reimagining Alzheimer's disease-an age-based hypothesis.J. Neurosci.*30*, 16755-16762.

Heusler, P. and Boehmer, G. (2007) Platelet-activating factor contributes to the induction of long-term potentiation in the rat somatosensory cortex *in vitro*. Brain Res *1135*, 85-91.

Hickman, S.E., Allison, E.K., and El Khoury, J. (2008) Microglial dysfunction and defective beta-amyloid clearance pathways in aging Alzheimer's disease mice. J Neurosci.*28*, 8354-8360.

Homma, H., Tokumura, A., and Hanahan, D. J. (1987) Binding and internalization of platelet activating factor 1-O-alkyl- 2-acetyl-sn-glycero-3-phosphocholine in washed rabbit platelets.J. Biol. Chem.*262*, 10582-10587.

Honda, Z., Ishii, S., and Shimizu T (2002) Platelet-activating factor receptor. J. Biochem. *131*, 773-779.

Honda, Z., Nakamura, M., Miki, I., Minami, M., Watanabe, T., Seyama, Y., Okado, H., Toh, H., Ito, K., Miyamoto, T., and Shimizu, T. (1991) Cloning functional expression of platelet activating factor receptor from guinea-pig lung. Nature. *349*, 342-346.

Honda, Z., Takano, T., Gotoh, Y., Nishida, E., Ito, K., and Shimizu, T. (1994) Transfected platelet-activating factor receptor activates mitogen-activated protein (MAP) kinase and MAP kinase kinase in Chinese hamster ovary cells. J. Biol. Chem.*269*, 2307-2315.

Hwang, S.B., Lam, M.H., and Shen, T.Y.(1985) Specific binding sites for platelet activating factor in human lung tissues.Biochem.Biophys. Res. Commun.*128*, 972-979.

Hwang, S.B. (1987) Specific receptor sites for platelet-activating factor on rat liver membranes. Arch. Biochim. Biophys.*257*, 339-344.

Hwang, S.B., Lee, C.S., Cheah, M.J., and Shen, T.Y. (1983) Specific receptor sites for 1-O-alkyl-2-O-acetyl-sn-glycero-3-phosphocholine (platelet activating factor) on rabbit platelet and guinea pig smooth muscle membranes. Biochemistry.*22*, 4756-4763.

Hwang, S.B., Lam, M.H., and Shen, T.Y. (1985) Specific binding sites for platelet-activating factor in human lung tissues. Biochem.Biophys. Res. Commun. *128*, 972-979.

Hwang, S.B., Lam, M.H., and Hsu, A.H. (1989) Characterization of platelet-activating factor (PAF) receptor by specific binding of [3H] L-659,989, a PAF receptor antagonist, to rabbit platelet membranes:possible multiple conformational states of a single type of PAF receptors. Mol. Pharmacol. *35,* 48-58.

Ishii, I., Izumi, T., Tsukamoto, H., Umeyama, H., Ui, M., and Shimizu, T. (1997) Alanine exchanges of polar amino acids in the transmembrane domains of a platelet-activating factor receptor generate both constitutively active and inactive mutants. J. Biol. Chem. *272*, 7846-7854.

Ishii, S., Kuwaki, T., Nagase, T., Maki, K., Tashiro, F., Sunaga, S., Cao, W.H., Kume, K., Fukuchi, Y., Ikuta, K., Miyazaki, J., Kumada, M., and Shimizu, T. (1998) Impaired anaphylactic responses with intact sensitivity to endotoxin in mice lacking a platelet activating factor receptor. J.Exp.Med. *187*, 1779-1788.

Ishii, S., Matsuda, Y., Nakamura, M., Waga, I., Kume, K., Izumi, T., and Shimizu, T. (1996) A murine platelet-activating factor receptor gene: cloning, chromosomal localization and up-regulation of expression by lipopolysaccharide in peritoneal resident macrophages. Biochem. J. *314*, 671-678.

Ishii, S., and Shimizu, T. (2000) Platelet-activating factor (PAF) receptor and genetically engineered PAF receptor mutant mice. Prog.Lipid. Res.*39*, 41-82.

Iivonen, H., Nurminen, L., Harri, M., Tanila, H., and Puoliväli, J. (2003) Hypothermia in mice tested in Morris water maze. Behav.Brain. Res.*141*, 207-213.

Iwata, N., Tsubuki, S., Takaki, Y., Shirotani, K., Lu, B., Gerard, N.P., Gerard, C., Hama, E., Lee, H.J., and Saido, T.C. (2001) Metabolic regulation of brain Abeta by neprilysin. Science.*292*, 1550-1552.

Izquierdo, I., Fin, C., Schmitz, P.K., Da Silva, R.C., Jerusalinsky, D., Quillfeldt, J.A., Ferreira, M.B.G., Medina, J.H., and Bazan, N.G. (1995) Memory enhancement by intrahippocampal, intraamygdala, or intraentorhinal infusion of platelet-activating factor measured in an inhibitory avoidance task. Proc. Natl. Acad. Sci. U S A. *92*, 5047-5051.

Izumi, T., and Shimizu, T. (1995) Platelet-activating factor receptor: gene expression and signal transduction. Biochim.Biophys.Acta.*1259*, 317-333.

Jarrett, J.T., Berger, E.P., and Lansbury, P.T. Jr. (1993) The carboxy terminus of the beta amyloid protein is critical for the seeding of amyloid formation: implications for the pathogenesis of Alzheimer"s disease. Biochemistry.*32*, 4693-4697.

Johnson, Z**.**, Power, C.A**.**, Weiss, C**.**, Rintelen, F**.**, Ji, H**.**, Ruckle, T**.**, Camps, M**.**, Wells, T.N**.**, Schwarz, M.K**.**, Proudfoot, A.E**.**, and Rommel, C. (2004) Chemokine inhibition--why, when, where, which and how? Biochem. So.c Trans.*32*, 366-377.

Kato, K., Clark, G.D., Bazan, N.G., and Zorunski, C.F. (1994) Platelet-activating factor as a potential retrograde messenger in CA1 hippocampal long-term potentiation.Nature.*367*, 175-179.

Kishimoto, S., Shimadzu, W., Izumi, T., Shimizu, T., Fukuda, T., Makino, S., Sugiura, T., and Waku, K. (1996) Regulation by IL-5 of expression of functional platelet-activating factor receptors on human eosinophils.J. Immunol.*157*, 4126-4132.

Klunk, W.F., Panchalingarn, K., McClure, R.J., and Pettegrew, J.W. (1996) Quantitative „H and "P MRS of PCA extracts of postmortem Alzheimer"s disease brain.Neurohiol.Aging.*17*, 349-357.

Klunk, W.E., Xu, C.J., McClure, R.J., Panchalingam, K., Stanley, J.A., and Pettegrew, J.W. (1997) Aggregation of beta-amyloid peptide is promoted by membrane phospholipid metabolites elevated in Alzheimer's disease brain. J. Neurochem. *69*, 266-272.

Kobayashi, K., Ishii, S., Kume, K., Takahashi, T., Shimizu, T., and Manabe, T. (1999) Platelet-activating factor receptor is not required for long-term potentiation in the hippocampal CA1 region. Eur. J. Neurosci. *11*, 1313-1316.

Kondratskaya, E.L., Pankratov, Y.V., Lalo, U.V., Chatterjee, S.S., and Krishtal, O.A. (2004) Inhibition of hippocampal LTP by ginkgolide B is mediated by its blocking action on PAF rather than glycine receptors. Neurochem. Int. *44*, 171-177.

Korth, R.M., Hirafuji, M., Benveniste, J., and Russo-Marie, F. (1995) Human umbilical vein endothelial cells: specific binding of plateletactivating factor and cytosolic calcium flux.Biochem.Pharmacol.*49*, 1793-1799.

Kotelevets, L., Noe,V., Bruyneel,E., Myssiakine,E., Chastre,E., Mareel,M. and Gespach,C. (1998) Inhibition by platelet-activating factor of Src- and hepatocyte growth factor-dependent invasiveness of intestinal and kidney epithelial cells. Phosphatidylinositol 3′-kinase is a critical mediator of tumor invasion. J. Biol. Chem., *273*, 14138-14145.

Kunievsky, B., and Yavin, E. (1994) Production and metabolism of platelet-activating factor in the normal and ischemic fetal rat brain.Crit.Care. Med. *30*, 294-301.

Kunz, D., Gerard, N.P., and Gerard, C. (1992) The human leukocyte platelet-activating factor receptor. cDNA cloning, cell surface expression, and construction of a novel epitope-bearing analog. J. Biol. Chem.*267*, 9101-9106.

Lee, T., Lenihan, D.J., Malone, B., Roddy, L.L., and Wasserman, S.I.(1984) Increased biosynthesis of platelet activating factor in activated human eosinophils.J. Biol. Chem. *259*, 5526-5530.

LeVan, T.D., Bloom, J.W., Adams, D.G., Hensel, J.L., and Halonen, M.(1998) Platelet-activating factor induction of activator protein-1 signaling in bronchial epithelial cells.Mol. Pharmacol.*53*, 135-140.

Ling, E.A., Kaur, L.C., Yick, T.Y., and Wong, W.C. (1990) Immunocytochemical localization of CR3 complement receptors with OX-42 in amoeboid microglia in postnatal rats. Anat. Embryol. (Berl).*182*, 481-486.

Ling, E.A. and Wong, W.C. (1993) The origin and nature of ramified and amoeboid microglia: a historical review and current concepts. Glia.*7*, 9-18.

Lotner, G.Z., Lynch, J.M., Betz, S.J., and Henson, P.M.(1980) Human neutrophil derived platelet activating factor. J. Immunol. *124*, 676-684.

Marcheselli, V.L., Rossowska, M.J., Domingo, M.T., Braquet, P., and Bazan, N.G. (1990) Distinct platelet-activating factor binding sites in synaptic endings and in intracellular membranes of rat cerebral cortex. J. Biol. Chem. *265*, 9140-9145.

Martins, I.C., Kuperstein, I., Wilkinson, H., Maes, E., Vanbrabant, M., Jonckheere, W., Van Gelder, P., Hartmann, D., D'Hooge, R., De Strooper, B., Schymkowitz, J., and Rousseau, F. (2008) Lipids revert inert Abeta amyloid fibrils to neurotoxic protofibrils that affect learning in mice. EMBO. J. *27*, 224-233.

Min, S.S., Quan, H.Y., Ma, J., Han, J.S., Jeon, B.H., and Seol, G.H. (2009) Chronic brain inflammation impairs two forms of long-term potentiation in the rat hippocampal CA1 area. Neurosci.Lett.*45,* 20-24.

Montrucchio, G., Alloatti, G., and Camussi, G.(2000) Role of platelet-activating factor in cardiovascular pathophysiology. Physiol. Rev. *80*, 1669-1699.

Mori, M., Aihara, M., Kume, K., Hamanoue, M., Kohsaka, S., Shimizu, T., Stephens, L., Jackson, T., and Hawkins, P.T. (1996) Predominant expression of platelet-activating factor receptor in the rat brain microglia. J. Neuroscie. *16*, 3590-3600.

Moriguchi, S., Shioda, N., Yamamoto, Y., and Fukunaga, K. (2010) Platelet-activating factor-induced synaptic facilitation is associated with increased calcium/calmodulin-dependent protein kinase II, protein kinase C and extracellular signal-regulated kinase activities in the rat hippocampal CA1 region. Neuroscience.*166*, 1158-1166.

Morris, R. (1984) Developments of a water-maze procedure for studying spatial learning in the rat.J. Neurosci. Methods.*11*, 47-60.

Mullen, R.J., Buck, C.R., and Smith, A.M.(1992) NeuN, a neuronal specific nuclear protein in vertebrates.Development.*116*, 201-211.

Mutoh, H., Bito, H., Minami, M., Nakamura, M., Honda, Z., Izumi, T., Nakata, R., Kurachi, Y., Terano, A., and Shimizu, T.(1993) Two different promoters direct expression of two distinct forms of mRNAs of human platelet-activating factor receptor. FEBS.Lett.*322*, 129-134.

Mutoh, H., Fukuda, T., Kitamaoto, T., Masushige, S., Sasaki, H., Shimizu, T., and Kato, S.(1996) Tissue-specific response of the human platelet-activating factor receptor gene to retinoic acid and thyroid hormone by alternative promoter usage.Proc. Natl. Acad. Sci. U S A.*93*, 774-779.

Nakamura, Y. (2002) Regulation Factors for Microglial Activation. Biol. Pharm. Bull. *25*, 945-953.

Nakao, A., Watanabe, T., Bitoh, H., Imaki, H., Suzuki, T., Asano, K., Taniguchi, S., Nosaka, K., Shimizu, T., and Kurokawa, K. (1997) cAMP mediates homologous downregulation of PAF receptor mRNA expression in mesangial cells. Am. J. Physiol.*273*, 445-450.

National Institute of Aging Alzheimer"s Disease Fact Sheet (2011)

Ninio, E., Mencia-Huerta, J.M., Heymans, F., and Benveniste, J.(1982) Biosynthesis of platelet activating factor. 1. Evidence for a acetyl-transferase activity in murine macrophages. Biochim.Biophys.Acta.*710*, 23-31.

Nitsch, R.M., Blusztajn, J.K., Pittas, A.G., Slack, B.F., Growdon, J.H., and Wurtman, R.J. (1992) Evidence for a membranedefect in Alzheimer disease brain. Proc. Nail. Acad. Sci. USA. *89*, 1671-1675.

O'Flaherty, J.T., Tessner, T., Greene, D., Redman, J.R., and Wykle, R.L. (1994) Comparison of 1-O-alkyl-, 1-O-alk-1′-enyl-, and 1-Oacyl- 2-acetyl-sn- glycero-3-phosphoethanolamines and -3-phosphocholines as agonists of the platelet-activating factor family. Biochim.Biophys.Acta.*1210*, 209-216.

O"Neil, C. (1992) Embryo-derived platelet activating factor. Reprod. Fertil.Dev. *4*, 283-228.

Ouellet, S., Müller, E., and Rola-Pleszczynski, M. (1994) IFN-γ up-regulates platelet-activating factor receptor gene expression in human monocytes. *J. Immunol.152*, 5092-5099.

Pettorossi, V.E. and Grassi, S. (2001) Different contributions of platelet-activating factor and nitric oxide in long-term potentiation of the rat medial vestibular nuclei.Acta.Otolaryngol. Suppl. *545*, 160-165.

Placanica, L., Zhu, L., and Li, Y.M. (2009) Gender- and age-dependent gamma-secretase activity in mouse brain and its implication in sporadic Alzheimer disease.PloS.ONE.*4*, 5088.

Prescott, S.M., McIntyre, T.M., Zimmerman, G.A., and Stafforini, D.M. (2002) Sol Sherry lecture in thrombosis: molecular events in acute inflammation. Arterioscler.Thromb.Vasc. Biol.*22*, 727-733.

Prescott, S.M., Zimmerman, G.A., Stafforini, D.M., and McIntyre, T.M. (2000) Platelet-activating factor and related lipid mediators.Annu. Rev. Biochem. *69*, 429-445.

Priller, C., Bauer, T., Mitteregger, G., Krebs, B., Kretzschmar, H.A., and Herms, J. (2006). Synapse formation and function is modulated by the amyloid precursor protein. J. Neurosci. *26*, 7212-7221.

Puglieli, L. (2002) Is ACAT a novel pharmacological target for the treatment of Alzheimer"s disease? Drugs Fut. *27*, 863.

Rademacher, T.W., Parekh, R.B., and Dwek, R.A.(1988) Glycobiology.Annu. Rev. Biochem.*57*, 785-838.

Raggers, R.J., Vogels, I., and van Meer, G. (2001) Multidrug-resistance P-glycoprotein (MDR1) secretes platelet-activating factor. Biochem. J.*357*, 859-865.
Ramnani, N. (2006) The primate cortico-cerebellar system: anatomy and function. Nat. Rev. Neurosci.*7*, 511-522.

Renooij, W., and Snyder, F. (1981) Biosynthesis of 1-alkyl-2-acetyl-sn-glycero-phosphocholine (platelet activating factor and a hypotensive lipid) by cholinephosphotransferase in various rat tissues. Biochim.Biophys.Acta.*663*, 545-556.

Righi, M., Letari, O., Sacerdote, P., Marangoni, F., Miozzo, A., and Nicosia, S. (1995) myc-immortalized microglial cells express a functional platelet-activating factor receptor. J. Neurochem. *64*, 121-129.

Ryan, S.D., Harris, C.S., Mo, F., Lee, H., Hou, S.T., Bazan, N.G., Haddad, P.S., Arnason, J.T., and Bennett, S.A. (2007) Platelet activating factor-induced neuronal apoptosis is initiated independently of its G-protein coupled PAF receptor and is inhibited by the benzoate orsellinic acid. J. Neurochem. *103*, 88-97.

Ryan ,S.D., Harris, C.S., Carswell, C.L., Baenziger, J.E., and Bennett, S.A. (2008) Heterogeneity in the sn-1 carbon chain of platelet-activating factor glycerophospholipids determines pro- or anti-apoptotic signaling in primary neurons. J. Lipid. Res.*49*, 2250-2258.

Ryan, S.D., Whitehead, S.N., Swayne, L.A., Moffat, T.C., Hou, W., Ethier, M., Bourgeois, A.J.G., Rashidian, J., P. Blanchard, A., Fraser, P.E., Figeys, D., Park, D.S., and Bennett, S.A.L. (2009) Amyloid-β42 signals tau hyperphosphorylation and compromises neuronal viability by disrupting alkylacylglycerophosphocholine metabolism. Proc. Natl. Acad. Sci. U S A. *106*, 20936-20941.

Saraf, M.K., Kishore, K., Thomas, K.M., Sharma, A., and Singh, M. (2003) Role of platelet activating factor in triazolobenzodiazepines-induced retrograde amnesia. Behav.Brain. Res. *142*, 31-40.

Sasaki, Y., Ohsawa, K., Kanazawa, H., Kohsaka, S., and Imai, Y. (2001) Iba1 is an actin-cross-linking protein in macrophages/microglia. Biochem.Biophys. Res. Commun.*286*, 292-297.

Sastre, M., Klockgether, T., and Heneka, MT. (2006) Contribution of inflammatory processes to Alzheimer's disease: molecular mechanisms.Int. J. Dev. Neurosci. *24*, 167-176.

Schubert, W., Prior, R., Weidemann, A., Dircksen, H., Multhaup, G., Masters, C.L., and Beyreuther, K. (1991) Localization of Alzheimer beta A4 amyloid precursor protein at central and peripheral synaptic sites. Brain. Res. *563*, 184-194.

Selkoe, D.J. (2001) Alzheimer's Disease: Genes, Proteins, and Therapy. Physiol. Rev. *81*, 741-766.

Sharma, S., Rakoczy, S., and Brown-Borg, H.(2010) Assessment of spatial memory in mice.Life. Sci.*87*, 521-536.

Shimada, A., Ota, Y., Sugiyama, Y., Sato, S., Kume, K., Shimizu, T., and Inoue, S. (1998). *In situ* expression of plate- let-activating factor (PAF)-receptor gene in rat skin and effects of PAF on proliferation and differentiation of cultured human keratinocytes. J. Invest. Dermatol.*110*, 889-893.

Shirasaki, H., Adcock, I.M., Kwon, O.J., Nishikawa, M., Mak, J.C., and Barnes, P.J. (1994) Agonist-induced up-regulation of platelet-activating factor receptor messenger RNA in human monocytes. Eur. J. Pharmacol. *268*, 263-266.

Shukla, S.D. (1992) Platelet-activating factor receptor and signal transduction mechanisms.FASEB. J. *6*, 2296-2301.

Simard, A.R. and Rivest, S. (2006) Neuroprotective properties of the innate immune system and bone marrow stem cells in Alzheimer's disease. Mol. Psychiatry. *11*, 327-335.

Simon, P., Dupuis, R., and Costentin, J., (1994) Thigmotaxis as an index of anxiety in mice. Influence of dopaminergic transmission. Behav.Brain. Res. *61*, 59-64.

Sisodia, S.S., Koo, E.H., Hoffman, P.N., Perry, G., and Price, D.L. (1993) Identification and transport of full-length amyloid precursor proteins in rat peripheral nervous system. J. Neurosci. *13*, 3136-3142.

Smale, S.T., and Baltimore, D. (1989) The "initiator" as a transcription control element. Cell.*57*, 103-113.

Smale, S.T., Schmidt, M.C., Berk, A.J., and Baltimore, D. (1990) Transcriptional activation by Sp1 as directed through TATA or initiator: specific requirement for mammalian transcription factor IID. Proc Natl. Acad. Sci. U S A.*87*, 4509-4513.

Snyder, F. (1987) Enzymatic pathways for platelet activating factor, related alkyl glycerolipids and their precursors. In: Platelet-Activating Factor and Related Lipid Mediators, edited by Snyder F. New York: Plenum.

Snyder, F. (1995) Platelet-activating factor and its analogs: metabolic pathways and related intracellular processes. Biochim.Biophys.Acta.*1254*, 231-249.

Sozzani, S., Longoni, D., Bonecchi, R., Luini,W., Bersani, L., D‟Amico, G., Borsatti, A., Bussolino, F., Allavena, P., and Mantovani, A. (1997) Human monocyte-derived and CD341 cell-derived dendritic cells express functional receptors for platelet activating factor. FEBS.Lett.*418*, 98-100.

Spencer, B., Marr, R.A., Rockenstein, E., Crews, L., Adame, A., Potkar, R., Patrick, C., Gage, F.H., Verma, I.M., and Masliah, E. (2008) Long-term neprilysin gene transfer is associated with reduced levels of intracellular Abeta and behavioral improvement in APP transgenic mice. BMC.Neurosci.*9*, 109.

Stoddart, N.R., Roudebush, W.E., and Fleming, S.D. (2001) Exogenous platelet-activating factor stimulates cell proliferation in mouse pre-implantation embryos prior to the fourth cell cycle and shows isoform-specific stimulatory effects. Zygote.*9*, 261-268.

Sugimoto, T., Tsuchimochi, H., McGregor, C. G., Mutoh, H., Shimizu, T. and Kurachi, Y. (1992) Molecular cloning and characterization of the platelet-activating factor receptor gene expressed in the human heart. Biochem.Biophys. Res. Commun. *189*, 617-624.

Sweet, R.A., Panchalingam, K., Pettegrew, J.W., McClure, R.J., Hamilton, R.L., Lopez, O.L., Kaufer, D.I., DeKosky, S.T., and Klunk, W.E. (2002) Psychosis in Alzheimer disease: postmortem magnetic resonance spectroscopy evidence of excess neuronal and membrane phospholipid pathology. Neurobiol.Aging.*23*, 547-553.

Takano, T., Honda, Z., Sakanaka, C., Izumi, T., Kameyama, K., Haga, K., Haga, T., Kurokawa, K., and Shimizu, T. (1994) Role of cytoplasmic tail phosphorylation sites of platelet-activating factor receptor in agonist-induced desensitization. J. Biol. Chem. *269*, 22453-22458.

Takano, T., Honda, Z., Watanabe, T., Uchida, S., Shimizu, T., and Kurokawa, K. (1991) Demonstration of platelet activating factor receptor in guinea pig kidney.Biochem.Biophys. Res. Common. *177*, 54-60.

Tanaka, T., Iimori, M., Tsukatani, H., and Tokumura, A. (1994) Platelet-aggregating effects of platelet-activating factor-like phospholipids formed by oxidation of phosphatidylcholines containing an sn-2-polyunsaturated fatty acyl group. Biochim.Biophys.Acta.*1210*, 202-208.

Tanzi, R.E., and Bertram, L. (2005). Twenty years of the Alzheimer‟s disease amyloid hypothesis: A genetic perspective. Cell.*120*, 545-555.

Tanzi, R.E., Moir, R.D., and Wagner, S.L. (2004) Clearance of Alzheimer's Abeta peptide: the many roads to perdition. Neuron.*43*, 605-608.

Teather, L.A., Packard, M.G., and Bazan, N.G. (1998) Effects of posttraining intrahippocampal injections of platelet-activating and PAF antagonists on memory.Neurobiol. Learn. Mem.*70*, 349-363.

Thal, D.R., Rüb, U., Schultz, C., Sassin, I., Ghebremedhin, E., Del Tredici, K., Braak, E., and Braak, H.(2000) Sequence of Abeta-protein deposition in the human medial temporal lobe. J Neuropathol. Exp. Neurol.*5*, 733-748.

Thivierge, M., Alami, N., Müller, E., de Brum-Fernandes, A.J., and Rola-Pleszczynski, M.(1993) Transcriptional modulation of platelet-activating factor receptor gene expression by cyclic AMP.J. Biol. Chem.*268*, 17457-17462.

Thivierge, M., Parent, J.L., Stankova, J., and Rola-Pleszczynski, M.(1996) Modulation of human platelet-activating factor receptor gene expression by protein kinase C activation.J. Immunol.*157*, 4681-4687.

Tokuoka, S.M., Ishii, S., Kawamura, N., Satoh, M., Shimada, A., Sasaki, S., Hirotsune, S., Wynshaw-Boris, A., and Shimizu, T. (2003) Involvement of platelet-activating factor and LIS1 in neuronal migration. Eur. J. Neurosci. *18*, 563-570.

Travers, J.B., Huff, J.C., Rola-Pleszczynski, M., Gelfand, E.W., Morelli, J.G., and Murphy, R.C. (1995) Identification of functional platelet-activating factor receptors on human keratinocytes. J. Invest. Dermatol.*105*, 816-823.

Traynor, B.J. and Singleton, A.B. (2010). Nature versus nurture: Death of a dogma, and the road ahead. Neuron.*68*, 196-200.

Triggiani, M., Schleimer, R.P., Warner, J.A., and Chilton, F.H.(1991) Differential synthesis of 1-acyl-2-acetyl-sn-glycero-3-phosphocholine and platelet-activating factor by human inflammatory cells. J. Immunol. *147*, 660-666.

Turner, P.R., O'Connor, K., Tate, W.P., and Abraham, W.C. (2003) Roles of amyloid precursor protein and its fragments in regulating neural activity, plasticity and memory.Prog.Neurobiol.*70*, 1-32.

van Biesen, T., Hawes, B.E., Raymond, J.R., Luttrell, L.M., Koch, W.J., and Lefkowitz, R.J. (1996) Go-protein a-subunits mediate Ras-independent MAP kinase activation. J. Biol. Chem. *271*, 1266-1269.

van Helvoort, A., Smith, A.J., Sprong, H., Fritzsche, I., Schinkel, A.H., Borst, P. and van Meer, G. (1996) MDR1 P-Glycoprotein is a lipid translocase of broad specificity, while MDR3 P-glycoprotein speci®cally translocates phosphatidylcholine. Cell.*87*, 507-517.

Vela, J.M., Dalmau, I.,González, B., and Castellano, B. (1995) Morphology and distribution of microglial cells in the young and adult mouse cerebellum. J. Comp. Neurol. *361*, 602-616.

Walsh, D.M., Hartley, D.M., Kusumoto, Y., Fezoui, Y., Condron, M.M., Lomakin, A., Benedek, G.B., Selkoe, D.J., and Teplow, D.B. (1999) Amyloid β-protein fibrillogenesis- Structure and biological activity of protofibrillar intermediates. J. Biol. Chem. *274*, 25945-25952.

Walsh, D.M., Tseng, B.P., Rydel, R.E., Podlisny, M.B., and Selkoe, D.J. (2000) The oligomerization of amyloid ß-protein begins intracellularly in cells derived from human brain. Biochemistry.*39*, 10831-10839.

Wang, X., Bae, J.H., Kim, S.U., and McLarnon, J.G. (1999) Platelet-activating factor induced Ca++ signaling in human microglia. Brain. Res. *842*, 159-165.

Wieraszko, A., Li, G., Kornecki, E., Hogan, M.V., and Ehrlich, Y.H. (1993) Long-term potentiation in the hippocampus induced by platelet- activating factor.Neuron.*10*, 553-557.

Wimo A, Prince M (2010) World Alzheimer Report 2010 The Global Economic Impact of Dementia. In: World Alzheimer Report (International AD, ed). Stockholm: Alzheimer's Disease International.

Wolfer, D.P., Stagljar-Bozicevic, M., Errington, M.L., and Lipp, H.P. (1998) Spatial memory and learning in transgenic mice: fact or artefact? News. Physiol. Sci. *13*,118-123.

Ye, R.D., Prossnitz, E.R., Zou, A.H., and Cochrane, C.G.(1991) Characterization of a human cDNA that encodes a functional receptor for platelet activating factor.Biochem.Biophys. Res. Commun.*180*, 105-111.

Zheng, H., Jiang, M., Trumbauer, M.E., Sirinathsinghji, D.J., Hopkins, R., Smith, D.W., Heavens, R.P., Dawson, G.R., Boyce, S., Conner, M.W., Stevens, K.A., Slunt, H.H., Sisoda, S.S., Chen, H.Y., and Van der Ploeg, L.H. (1995) beta-Amyloid precursor protein-deficient mice show reactive gliosis and decreased locomotor activity. Cell.*81*, 525 -531.

Zheng, H. and Koo, E.H. (2006)The amyloid precursor protein: beyond amyloid. Mol. Neurodegener. *3*, 1-5.

Zhu, Y.P., Word, R.A., and Johnston, J.M. (1992)The presence of platelet-activating factor binding sites in human myometrium and their role in uterine contraction. Am. J. Obstet. Gynecol. *166*, 1222-1228.

Zhou SJ, Zhu ME, Shu D, Du XP, Song XH, Wang XT, Zheng RY, Cai XH, Chen JF, and He JC.(2009) Preferential enhancement of working memory in mice lacking adenosine A(2A) receptors. Brain. Res.*1303*, 74-83.

CURRICULUM VITAE

VIAN PESHDARY

1181 County Rd. 26 613-761-2766
Plantagenet, ON, K0B 1L0
peshdaryv@gmail.ca

Education

MSc. Biochemistry
University of Ottawa, Ottawa, ON
Sept 2009 – Dec 2011

BSc. Biochemistry
University of Ottawa, Ottawa, ON
May 2009

Previous Employment

Head Teacher's Assistant (TA), Ottawa University *(1/2010-4/2010)*
Ottawa, Ontario: Department of Biochemistry
Trained other TA's and overlooked the laboratory sessions, prepared a consensus laboratory report marking scheme, lab demonstrator, mentored undergraduate students in biochemical techniques, evaluated laboratory reports and laboratory performance

Teacher's Assistant (TA), Ottawa University *(1/2009-4/2009)*
Ottawa, Ontario: Department of Biochemistry
Lab demonstrator, mentored undergraduate students in biochemical techniques, evaluated laboratory reports and laboratory performance

Teacher for Minicourse, Ottawa University *(4/2010-5/2010)*
Ottawa, Ontario: Department of Biochemistry *(4/2009-5/2009)*
Lab demonstrator, taught basic biochemistry to gifted *(4/2008-5/2008)*
Elementary and high school students taking a biochemistry *(4/2007-5/2007)*
mini enrichment course offered at the University of Ottawa

Laboratory Technician, Ottawa University *(10/2006-4/2009)*
Ottawa, Ontario; Steffany Bennett Lab
Genotyped and handled various mouse colonies, performed animal work for graduate students, carried on individual projects and laboratory tasks

Supervisor/ Cashier, Metro (Loeb) Inc. *(8/2003-1/2007)*
Ottawa, Ontario
Operated the cash register, handled money, opened and closed the store, conducted various store related paper and computer work, supervised 6 – 8 cashiers during a single shift

Comic Illustrator, private client *(4/2006-5/2007)*
Ottawa, Ontario
Illustrated a story board for the movie project, *A Walk in the Light*

Wall Illustrator, private client *(1/2006-5/2007)*
Ottawa, Ontario
Designed, illustrated, and painted walls of nursery rooms

Scholarships

University of Ottawa Biochemistry, Microbiology and Immunology Soft-Funded Scholarship
(2009- 2011)

University of Ottawa Entrance Scholarship
(2004)

Queen Elizabeth II Reaching For the Top Scholarship, ON
(2004)

Publication

Kennedy KAM, Porter T, Mehta V, Ryan SD, Price F, **Peshdary V**, Karamboulas C, Savage J, Drysdae T, Li S-C, Bennett SAL, Skerjanc IS. (2009) Retinoic acid can enhance skeletal muscle specification and bypass inhibition by Bone Morphogenetic Protein 4 but not by dominant negative beta-catenin**.** BMC Biology, 7: 67.

Graduate Courses Completed

BCH 8105. Advanced Topics in the Molecular Biology of Human Diseases
University of Ottawa, Completed Winter 2011
Mark: A

BCH8310. Current Topics in RNA Molecular Biology
University of Ottawa, Completed Fall 2010
Mark: A-

ARCC5003. Design and Technology Workshop
Carleton University, Completed Winter 2010
Mark: A-

NSC5102. Cellular and Molecular Neuroscience
University of Ottawa, Completed Fall 2009
Mark: A-

Laboratory Skills

Molecular Genetics: Genetic cloning (PCR, RT – PCR, ligation, restriction enzyme digests, recombination, transformation), primer design and optimization, DNA and RNA purification, plasmid amplification (MINI preps), *in situ* hybridization, immunofluorescence staining of frozen tissue

***In Vivo* Work:** Mouse perfusion, mouse brain (hippocampus, posterior cortex, etc.) dissection, mouse body (heart, lung, and liver) dissection, mouse brain sectioning, mouse brain synaptosome extraction and purification, Morris water Maze (MWM) behavior analysis

Proteomic and Lipidomic: Western blotting, protein and lipid extraction, TUNEL assay

Microscopy: Light microscopy and Fluorescent microscopy

Computing: Photoshop, Clone Manager**,** Graph Pad In Stat, Graph Pad Prism, Delta Graph**,** Pymol**,** Fly Lab**,** Microsoft word and Microsoft Excel**,** Endnote**,** Autodesk Maya and Adobe Premiere Pro CS4